Air Force Institute of Technology

AFIT Scholar

3-5-2007

Sub-Surface Navigation Using Very-Low Frequency Electromagnetic Waves

Alan L. Harner

Follow this and additional works at: https://scholar.afit.edu/etd

Part of the Electromagnetics and Photonics Commons

SUB-SURFACE NAVIGATION
USING VERY-LOW FREQUENCY
ELECTROMAGNETIC WAVES

THESIS

Alan L. Harner, 1st Lieutenant, USAF

AFIT/GE/ENG/07-12

DEPARTMENT OF THE AIR FORCE
AIR UNIVERSITY

AIR FORCE INSTITUTE OF TECHNOLOGY

Wright-Patterson Air Force Base, Ohio

AFIT/GE/ENG/07-12

SUB-SURFACE NAVIGATION
USING VERY-LOW FREQUENCY
ELECTROMAGNETIC WAVES

THESIS

Presented to the Faculty

Department of Electrical and Computer Engineering

Graduate School of Engineering and Management

Air Force Institute of Technology

Air University

Air Education and Training Command

In Partial Fulfillment of the Requirements for the

Degree of Master of Science in Electrical Engineering

Alan L. Harner, B.S.E.E.

1st Lieutenant, USAF

March 2007

APPROVED FOR PUBLIC RELEASE; DISTRIBUTION UNLIMITED.

SUB-SURFACE NAVIGATION
USING VERY-LOW FREQUENCY
ELECTROMAGNETIC WAVES

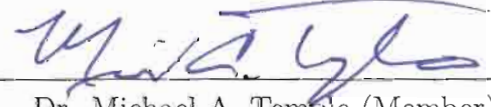Alan L. Harner, B.S.E.E.

1st Lieutenant, USAF
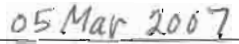
Approved:

Dr. John F. Raquet (Chairman)	5 MAR 2007
	date
Dr. Michael A. Temple (Member)	5 Nov 07
	date
Dr. Michael J. Havrilla (Member)	05 Mar 2007
	date

Abstract

The ability to navigate in all environments has become very valuable for many applications, and there is a growing desire to navigate underground. Traditional navigation methods such as the Global Positioning System (GPS) do not work underground due to increased attenuation of high frequency navigation signals as they propagate through the earth. This research proposes two schemes utilizing very-low frequency (VLF) electromagnetic waves (3 kHz to 10kHz) to navigate underground.

The first scheme consists of using above-ground beacon transmitters to broadcast VLF signals to an underground mobile receiver. This method uses triangulation and trilateration to obtain a position solution. The second scheme consists of using above-ground reference receivers along with an underground mobile receiver. In this case, time-difference-of-arrival measurements are formed using VLF signals of opportunity, such as lightning strike emissions, and used to calculate a position solution.

The objective of this thesis is to develop positioning algorithms and use simulations to characterize the effects that varying parameters such as measurement errors, measurement type, number of measurements, transmitter/reference receiver location, mobile receiver position, and material constant errors have on position solution accuracy. This is accomplished using a Monte Carlo analysis of nine trade studies which vary a major parameter over a range of accepted values.

Although simplifying assumptions are made to limit the research scope, the results show trends that would still be expected using more complex methods and models. The positioning algorithms varied depending on the type of measurement used; the raw power vector measurements or converted length and difference angle measurements. The resulting trend suggests that choosing the appropriate measurement type and transmitter/reference receiver geometry have a dramatic effect on the accuracy of the mobile receiver's position solution.

Acknowledgements

Above all, I would like to thank my wife for her love and support; her patience and understanding. She pushed me to achieve things I never thought possible. Without her, I would not be where I am today and I am eternally grateful.

I would also like to thank my thesis advisor, Dr. John Raquet, for his expert guidance and letting me make something I can truly be proud of. Finally, I would like to thank the committee members for their subject matter knowledge, their willingness to help, and taking the time out of their busy schedules to offer constructive feedback.

Alan L. Harner

Table of Contents

List of Figures

List of Tables

SUB-SURFACE NAVIGATION

USING VERY-LOW FREQUENCY

ELECTROMAGNETIC WAVES

I. Introduction

The ability to navigate in all environments has become very valuable for many applications, and there is a growing desire to be able to navigate underground. Whether for cave rescue, surveying, or infiltrating an underground enemy base, knowing one's position is essential. Traditional navigation methods such as the Global Positioning System (GPS) do not work underground, due to the attenuation of high frequency navigation signals as they propagate through the earth. The high frequency nature of GPS signals only allows them to penetrate the ground approximately 2 inches [9]. Therefore, alternative approaches must be found for underground navigation.

The distance an electromagnetic wave can propagate underground is based largely on three factors: the material through which it propagates, the transmission power, and its frequency. Of the three, the material through which the wave is propagating is the only factor that cannot be changed, since it is determined by the environment which must be navigated. To some extent the earth's composition can be predicted and modelled to help account for various errors, but it cannot be changed. However, the other two factors of frequency and power can be exploited to navigate underground. This thesis proposes two schemes for doing so.

The first scheme is a direct manipulation of the two exploitable factors by using transmitters to broadcast at a particular frequency and power. While the power output is limited due to technical issues such as antenna size and transmitter battery capacity, the frequency component can sweep across the entire electromagnetic spectrum. However, the very-low frequency (VLF) range (3 kHz to 30 kHz) that will

1

allow the transmission wave to propagate the furthest through the earth. As multiple transmitters are placed in a coverage area, a mobile receiver underground can gather these signals and use techniques such as triangulation and multi-lateration similar to GPS to create a position solution.

The second scheme involves using existing VLF signals of opportunity to create a position solution. A network of reference receivers is setup to listen for various signals within the desired frequency range. As a signal of opportunity propagates through the network, a mobile receiver within the network uses a mobile to reference time-difference-of-arrival technique to find a relationship between it and the reference receivers. This relationship places the mobile receiver somewhere on a line parallel to the signal of opportunity wavefront. As subsequent signals pass through the network, additional lines are created. The mobile receiver can then find its position based on an intersection of these lines using weighted least squares.

1.1 *Problem Statement*

The objective of this thesis is to develop positioning algorithms and use simulations to characterize the effects that varying parameters such as measurement errors, measurement type, number of measurements, transmitter/reference receiver location, mobile receiver position, and material constant errors have on the position solution accuracy. This is accomplished using a Monte Carlo analysis of nine trade studies which varies a major parameter over a range of accepted values.

1.2 *Assumptions*

Simplifying assumptions are needed to focus the research in a direction so that conclusions can be reached without making the simulations overly complex, i.e. several assumptions must be made to limit the scope of the research.

- Simple Media: The media through which electromagnetic signals propagate are considered linear, isotropic, and homogenous; therefore, all second and higher-

2

order effects are removed. This assumption is made to simplify calculations and is not a feasible assumption for actual system operation.

- White, Gaussian Noise: Unless specifically called out as a bias, all error sources are assumed to be white and Gaussian.

- Measurement Availability: All measurements and transmitters/receivers that generated the measurements are known, i.e., they have been tagged with the appropriate transmitter/receiver. The measurements have been sent through an antenna/sensor and other related hardware and converted to a measurement vector or time for use in the simulation.

- Clock Errors Neglected: The clock errors for the second scheme are neglected and considered synchronous with GPS time. For an actual system using timing, estimation of clock errors is needed to account for the imperfections in the hardware clocks. This assumption is made for simplicity and the clock errors would need to be properly estimated for an actual system.

1.3 Related Topics and Research

This section describes topics and research related to the thesis. It is broken into three categories of interest: underground navigation, beacon navigation, and signals of opportunity navigation.

1.3.1 Underground Navigation. The first category of underground navigation presents two methods for achieving a position solution underground: cave radiolocation and a magnetic sensor sheet.

1.3.1.1 Cave Radiolocation. Cave radiolocation is a technique used to determine the horizontal position and vertical depth of an underground radio transmitter. A Very Low Frequency (VLF) signal is transmitted by an underground horizontally oriented loop antenna. A radio receiver above ground measures the field strength of the transmitted wave. The receiver loop can be oriented in a way such
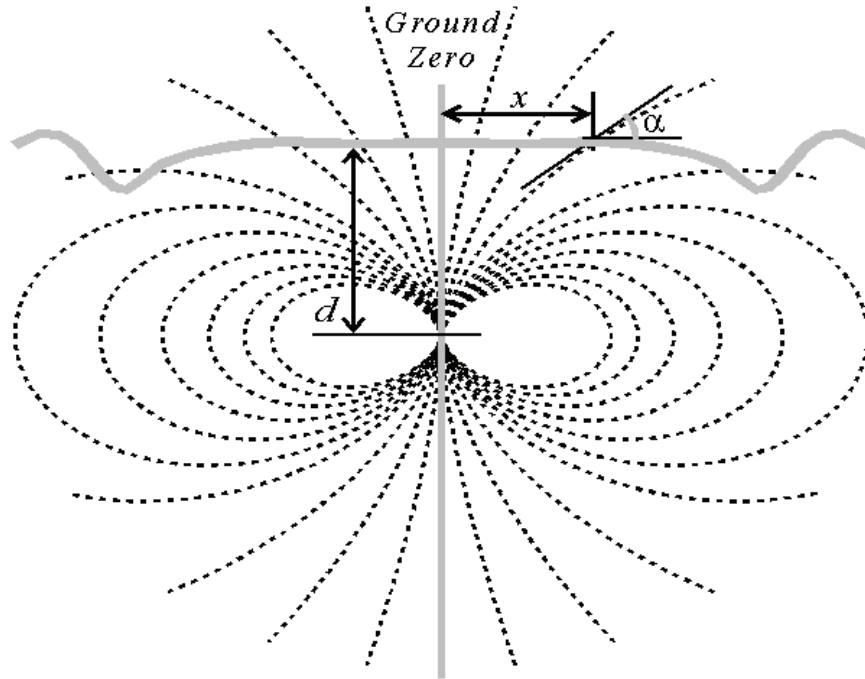
Figure 1.1:   The magnetic field lines from an underground transmitter.

that no signal is received, or a 'null' is found. The operator can triangulate several nulls to find the 'ground zero' point directly above the underground transmitter. Using GPS, the underground transmitter's horizontal position can be estimated. Two methods of determining the depth of the underground transmitter can be used. One is to accurately measure the field strength above ground and calculate the depth based on how much the signal has decayed. The second method is to take measurements at a distance x from 'ground zero' as shown in Figure 1.1. The angle a of the field line can be used to determine a distance d from 'ground zero' to the underground transmitter. Several data points are used to find a best fit solution [4].

1.3.1.2   Magnetic Sensor Sheet.   This approach has been used to find the position of an underground tunnelling robot at a depth of 3 to 5 m. A 7' x 9', 1.3 mm thick sheet composed of array of 63 highly sensitive magnetometers is laid over the area to be navigated. A transmitting coil is installed on the tunnelling robot head and produces a 220 Hz magnetic field. The sensor array reads the transmitted signal

field strength. Since the sensors are separated by 1 foot, the data is interpolated to find the peak of the electromagnetic field. The robot's horizontal position is estimated to be the location of this peak with an accuracy of less than 8mm for each axis [10].

1.3.2 Beacon Navigation. Since the first scheme uses transmitter beacons to find a position solution, it is useful to review this category of beacon navigation systems that employ the use of beacons to generate a position solution: LORAN and the Distributed Magnetic Local Positioning System.

1.3.2.1 LORAN. LOng RAnge Navigation was developed for use as a maritime and aircraft radiolocation navigation system near coastal areas of the United States. Multiple transmitter stations synchronized in time broadcast a very low frequency signal that is picked up by a mobile radio receiver. A time-difference-of-arrival measurement is formed between each signal broadcasted, placing the mobile on hyperbolic solution lines. The mobile radio's position is then calculated as the intersection of all the resulting hyperbolas [5].

1.3.2.2 Distributed Magnetic Local Positioning System. The system presented in [8] uses multiple beacons distributed throughout a building to determine the position and attitude of a mobile robot. The beacons are at known locations, transmit at a known power, use an orthogonal set of pseudo-random codes, and operate an extremely-low frequency (10 Hz) magnetic field to distinguish one beacon from another. A receiver on the mobile robot measures the field strength at it's current location. Since the beacons use a pseudo-random code when transmitting, the field strengths associated with each beacon can be extracted from the measurements. Now the robot can determine it's distance from a particular beacon based on known characteristics of the electromagnetic field produced by each beacon. Once all the distances are found, the position of the robot can be determined with an accuracy of 2.4 *cm*.

1.3.3 Signals of Opportunity Navigation. The second scheme in this research uses signals of opportunity as a basis for navigation. Details are found in two research papers focused on using a certain signal of opportunity to create a position solution: the NTSC Broadcast Signal and the AM Transmission Band.

1.3.3.1 NTSC Broadcast Signal. Eggert evaluated the navigation potential of the National Television System Committee (NTSC) broadcast signal. Time-difference-of-arrival (TDOA) measurements were created using the NTSC broadcast signals collected from low and high multipath environments. Three data reduction algorithms were used to evaluate the severity and dynamic effects of NTSC broadcast multipath signals for each environment. The simulations created using these algorithms revealed a 40m position accuracy with the typical range errors found during initial testing [3].

1.3.3.2 AM Transmission Band. McEllroy evaluated the navigation potential of the Amplitude Modulated (AM) band of the electromagnetic spectrum (520 to 1710 kHz). Using time-difference-of-arrival (TDOA) of an AM signal between a reference receiver and mobile receiver, a position solution could be found if the source locations of the AM signals were known. A simulation was created to evaluate the performance of the proposed hardware system. In an attempt to model real-world AM signal characteristics, four methods were developed to estimate the cross-correlation peak within a specified portion of data. Each method was used in the simulation to evaluate that method's effect on the position solution. The simulations produced sub-meter level accuracies before large errors were introduced. Hardware problems arose during the real-world implementation and more sophisticated hardware is required for further testing [7].

1.4 Thesis Overview

Chapter 2 provides background information and presents concepts pertinent to this research. These concepts include electromagnetic theory and various posi-

tion solution methods. Chapter 3 gives a detailed look at the simulations created in MATLAB® for this research. Block diagrams of the parameters, truth model, generated and converted measurements, and solution methods for each of the two simulations are described. Chapter 4 presents the results and analysis for the nine trade studies called out in the problem statement above. Chapter 5 gives a summary of the trade study results and make recommendations for future research pertaining to this thesis.

II. Background

This chapter presents the background topics fundamental to this research. First, a basic theory of electromagnetic wave propagation will be explained. Second, an overview of elementary geometry is given as a basis for the underlying positioning concepts. These concepts are then explored in greater detail in a positioning overview. Typical errors which are found in this research are then defined. Next, the least squares estimation technique is addressed. Finally, signals of opportunity are introduced and examples are given.

2.1 Electromagnetic Wave Propagation Overview

Since this thesis focuses on using very-low frequency electromagnetic waves to navigate underground, an understanding of the basic concepts is essential. The following sections explain electromagnetic wave propagation theory in its most basic form. Maxwell's equations are given in full and then simplified to be useful as a mathematical tool.

2.1.1 Material Constants.   All materials have properties intrinsic to them. Some properties deal with temperature while others deal with electromagnetic wave propagation through the media. Three important electromagnetic wave propagation properties are conductivity, permeability, and permittivity. Although these properties can vary with time, temperature, and frequency, in a linear, homogenous, and isotropic media they remain constant for a constant frequency [1].

2.1.1.1 Conductivity.   Conductivity is a proportionality constant, σ, relating the average drift velocity, $\mathbf{J}$, to the electric field intensity, $\mathbf{E}$:

$$\mathbf{J} = \sigma\mathbf{E} \qquad (2.1)$$

Conductivity is a measure of how susceptible a material is to supporting a conduction current when an electric field is present. It is the reciprocal of resistivity, so a good conductor such as copper would have a high conductivity.

2.1.1.2 Permeability. Permeability is another proportionality constant, μ, that relates the magnetic field intensity, $\mathbf{H}$, to the magnetic flux density, $\mathbf{B}$, as shown:

$$\mathbf{H} = \frac{1}{\mu}\mathbf{B} \qquad (2.2)$$

Permeability is a measure of how susceptible a material is to becoming magnetized when a magnetic field is present. The parameter μ is known as the absolute permeability which is a function of the permeability of free space, μ_0, and the relative permeability of the media, μ_r, where:

$$\mu = \mu_0\mu_r \qquad (2.3)$$

2.1.1.3 Permittivity. Permittivity is also a proportionality constant, ϵ, relating the electric flux density, $\mathbf{D}$, to the electric field intensity, $\mathbf{E}$, as follows:

$$\mathbf{D} = \epsilon\mathbf{E} \qquad (2.4)$$

Permittivity is a measure of how susceptible a material is to becoming electrically polarized when an electric field is present. The parameter ϵ is known as the absolute permittivity which is a function of permittivity of free space, ϵ_0, and the relative permittivity of the media, ϵ_r, where:

$$\epsilon = \epsilon_0\epsilon_r \qquad (2.5)$$

2.1.2 Maxwell's Equations. James Clerk Maxwell developed four consistent equations that form the foundation of all electromagnetic theory. They are as follows:

$$\nabla \times \mathbf{E} = -\frac{\partial \mathbf{B}}{\partial t} \tag{2.6}$$

$$\nabla \times \mathbf{H} = \mathbf{J} + \frac{\partial \mathbf{D}}{\partial t} \tag{2.7}$$

$$\nabla \cdot \mathbf{D} = \rho \tag{2.8}$$

$$\nabla \cdot \mathbf{B} = 0 \tag{2.9}$$

Although these four equations are consistent, they are not independent. Each of the fundamental field vectors **E, H, D, B** have three component vectors. Together they produce twelve unknowns and require twelve scalar equations to solve. In order to find a solution, simplifications are made. In a linear, homogenous, and isotropic media, the constitutive relations from Section 2.1.1, $\mathbf{D} = \epsilon \mathbf{E}$ and $\mathbf{H} = \frac{1}{\mu}\mathbf{B}$, bring about substitutions in Maxwell's equations and reduce the number of scalar equations needed by six leaving six equations with six unknowns, which is a solvable linear system [1].

2.1.3 Skin Depth. As an electromagnetic wave propagates through a media, the signal strength is attenuated [1]. The amount of attenuation is based on the frequency, f, and the material constants μ and σ. The attenuation factor, α, and the depth, z, give an attenuation rate of $e^{-\alpha z}$ so the amplitude of the wave will be attenuated by a factor of $e^{-1} \approx 0.368$ when it travels a distance of $\delta = \frac{1}{\alpha}$ [?]. This distance is called the skin depth or depth of penetration. For a simple, conductive media, $\alpha = \sqrt{\pi f \mu \sigma}$ which gives rise to the simplified skin depth formula used in this research:

$$\delta_{SD} = \frac{1}{\sqrt{\pi f \mu \sigma}} \tag{2.10}$$

2.2 Elementary Geometry Overview

The following sections aid in visualizing and deriving the underlying concepts needed to create a position solution.
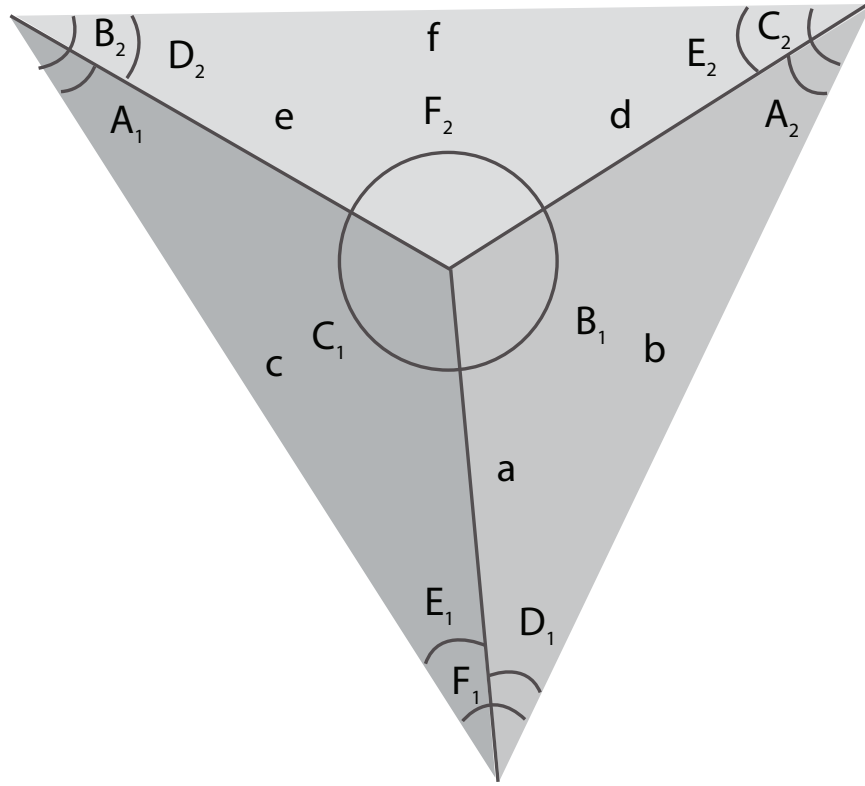
Figure 2.1:   A regular tetrahedron.

2.2.1   Tetrahedron.   A tetrahedron is a four-sided polyhedron with six edges. Each face is a triangle with an edge that is common to at most one other face. Figure 2.1 is an example of a regular tetrahedron (all faces and sides are equal). The triangles that compose the faces must adhere to the basic triangle equations such as the Law of Sines and the Law of Cosines. Figure 2.2 shows a reference triangle with sides **a,b,c** and angles **A,B,C** for the following Laws:

$$Law\ of\ Sines: \quad \frac{a}{\sin A} = \frac{b}{\sin B} = \frac{c}{\sin C} \tag{2.11}$$

$$Law\ of\ Cosines: \quad \cos A = \frac{-a^2 + b^2 + c^2}{2bc} \tag{2.12}$$

$$\cos B = \frac{-b^2 + a^2 + c^2}{2ac} \tag{2.13}$$

$$\cos C = \frac{-c^2 + a^2 + b^2}{2ab} \tag{2.14}$$

11
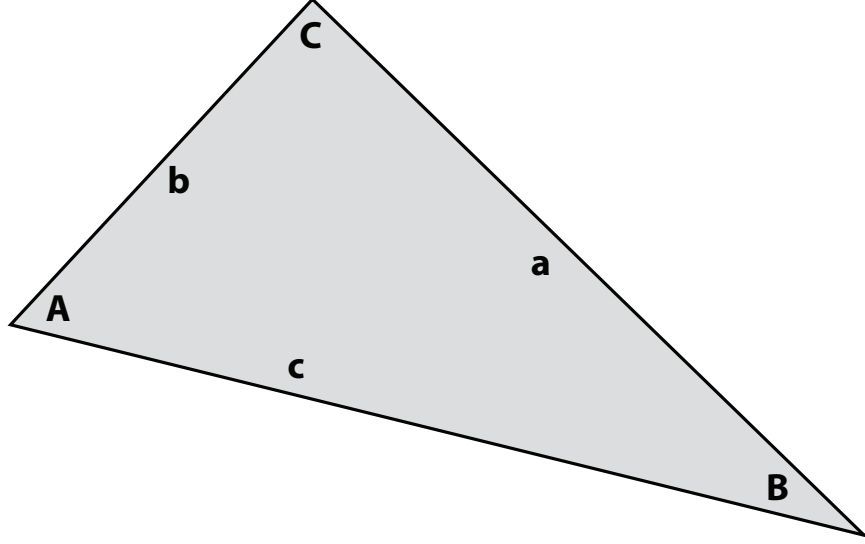
Figure 2.2:   A reference triangle.

To find a unique solution to a triangle, one must know 1) at least three out of the six variables that define a triangle ($\mathbf{a,b,c,A,B,C}$) and 2) at least one side's length. To find a unique solution for a tetrahedron ($\mathbf{a,b,c,d,e,f}$) as shown in Figure 2.1, all four triangles must be solved for. Each triangle has an edge in common with it's neighbor resulting in six edges. Using the Law of Sines and the Law of Cosines, the following closed-form relationship can be derived:

$$V a^2 + (WT + XU)a - (ZTU + Y) = 0 \qquad (2.15)$$

where:

$T = \sqrt{\frac{d^2}{\sin D_1{}^2} - a^2}$

$U = \sqrt{\frac{f^2}{\sin F_1{}^2} - a^2}$

$V = 2(\cos D_1^2 + \cos F_1^2 - 1 - \cos D_1 \cos E_1 \cos F_1)$

$W = 2(\cos D_1 - \cos E_1 \cos F1)\sin D_1$

$X = 2(\cos F_1 - \cos D_1 \cos E_1)\sin F_1$

$Y = d^2 + f^2 - e^2$

$Z = 2\cos E_1 \sin D_1 \sin F_1$

This shows that if triangle $\mathbf{d,e,f}$ can be completely defined and if the angles $\mathbf{D_1, E_1, F_1}$

that are opposite these sides are known, then side **a** can be solved for through an iterative method.

2.2.2 Slope Intercept Form. A line $\overleftrightarrow{\mathbf{AB}}$ can be uniquely determined by two points (x_1, y_1) and (x_2, y_2). The line can be defined as:

$$y - y_1 = \frac{y_2 - y_1}{x_2 - x_1}(x - x_1) \tag{2.16}$$

where

$\frac{y_2 - y_1}{x_2 - x_1}$ is the slope m of the line

Unless the line is completely horizontal or vertical, it has both an x- and y-intercept. Horizontal lines only have a y-intercept while vertical lines only have an x-intercept. For non-vertical lines, a point-slope intercept form can be made. The y-intercept can be found as follows:

$$b = -mx_1 + y_1 \tag{2.17}$$

which yields the slope intercept form of a line:

$$y = mx + b \tag{2.18}$$

2.2.3 3-Dimensional Line Intersection. The lines discussed in the previous section were two-dimensional. A line in three dimensions is also uniquely defined with two points (x_1, y_1, z_1) and (x_2, y_2, z_2). The equations for the line passing through the point (x_0, y_0, z_0) that is parallel to a nonzero vector $\overrightarrow{abc}$ can be expressed parametrically as:

$$x = x_0 + at \tag{2.19}$$

$$y = y_0 + bt \tag{2.20}$$

$$z = z_0 + ct \tag{2.21}$$

13

The intersection point $a = (x, y, z)$ of two such lines containing points $a_1 = (x_1, y_1, z_1)$, $a_2 = (x_2, y_2, z_2)$, $a_3 = (x_3, y_3, z_3)$, and $a_4 = (x_4, y_4, z_4)$ can be solved with a linear system of equations given by:

$$\mathbf{a} = \mathbf{a_1} + (\mathbf{a_2} - \mathbf{a_1})t_1 \tag{2.22}$$

$$\mathbf{a} = \mathbf{a_3} + (\mathbf{a_4} - \mathbf{a_3})t_2 \tag{2.23}$$

2.3 Positioning Overview

Finding a position solution is the key to this research. Three important solution methods in positioning are triangulation, trilateration, and time-difference-of-arrival.

2.3.1 Triangulation. In Section 2.2.1, finding a unique solution to a triangle was discussed. One must know three out of the six variables, (**a**,**b**,**c**,**A**,**B**,**C**), to define a triangle, one of which is the length of a side. For triangulation, two of the three variables known are angles and the third is a length, as shown in Figure 2.3. For two given angles **A** and **B**, the third angle **C** is simply $180 - \mathbf{A} - \mathbf{B}$. With one known length, the lengths of the remaining two sides can then be found using the Law of Sines. In positioning, this is useful when coordinates of two reference points **a** and **b** are known. To find a third unknown coordinate **c**, triangulation can be used if the angle **A** at point **a** between the unknown point **c** and the opposite reference point **b** can be found as shown in Figure 2.3. The distance, l, between the two reference points can be calculated for the one known length. This can be extended to the 3-dimensional case wherein the geometry of the tetrahedron is used. Now three reference points are needed as well as all angles formed between the unknown point and opposite reference points.

2.3.2 Trilateration. Trilateration is similar to triangulation but instead of using two angles and one side length to find the unknown point **c**, three known lengths are used. Using various methods, the distance or length between both reference points **a** and **b** and the unknown point **c** can be found. However, on a 2-D plane, there are

14
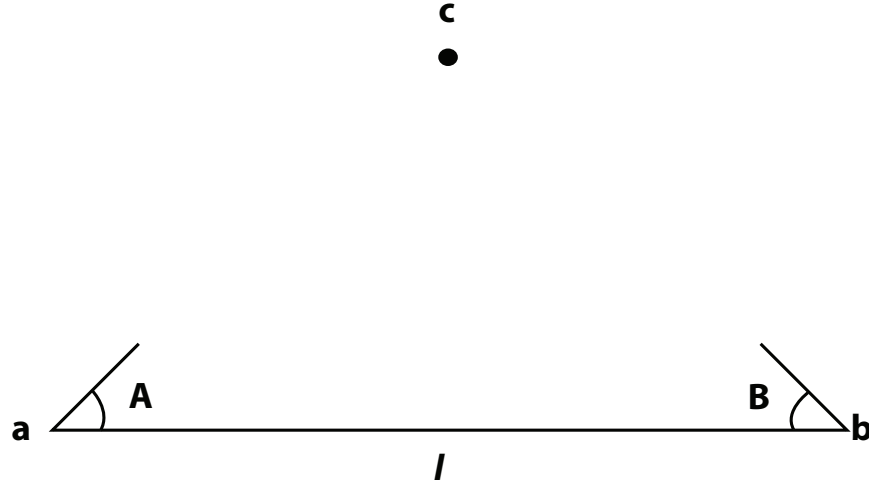
Figure 2.3:   The method of triangulation. The angles **A** and **B** are formed between the unknown point **c** and the opposite reference point. With a known length l, the unknown point **c** can be found.

two possible solutions for the unknown point **c** shown as $\mathbf{p_1}$ and $\mathbf{p_2}$ in Figure 2.4. A third reference point **d** which also intersects with $\mathbf{p_1}$ must be used to uniquely identify a solution. To extend this three dimensions, a fourth reference point must be used to solve for a unique, unambiguous solution.

2.3.3   Time-Difference-of-Arrival.   Time-difference-of-arrival (TDOA) is one method used to find a receiver's position. In a time synchronous system, a signal can be sent from one location at an initial time t_0 and then received at another location at time t_1. The time of travel is then:

$$t_1 - t_0 \tag{2.24}$$

This time of travel is then multiplied by the speed of signal (the speed of light for radio signals in free space) to get a distance or length. If there are outside sources being received by a reference and a mobile receiver, then the time difference between when they both received the signal is the time-difference-of-arrival. This time difference can then be used to place the mobile receiver on a hyperbola extending from the

15
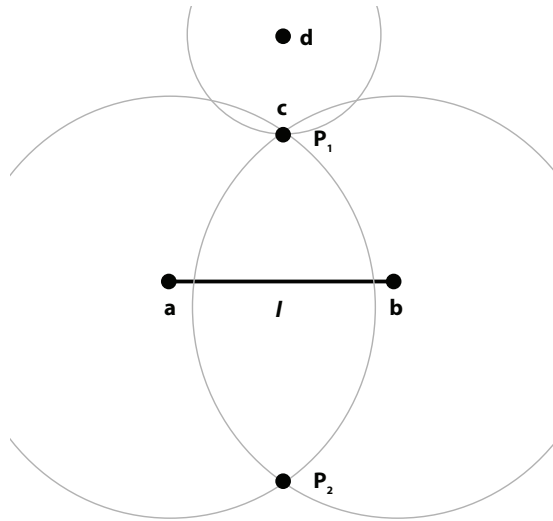
Figure 2.4: The method of trilateration. Three reference points (**a**, **b**, and **d**) must be known to uniquely identify an unknown position **c**.

source. As multiple sources are added, additional hyperbolas are formed. The mobile receiver's position is then the intersection of these hyperbolas.

2.4 *Typical Errors*

Identifying and accounting for error sources is essential to the accuracy of a given solution. Typical errors that affect underground navigation are summarized here.

2.4.1 Electromagnetic Propagation Effects. There are a number of second and higher-order effects such as bending and attenuation that occur to an electromagnetic wave as it passes through the earth. The incoming measurements to the mobile receiver come in the form of a three-dimensional raw power vector, $\mathbf{P}$. These electromagnetic propagation effects can skew the raw power vector direction and/or magnitude. Although a simple media is used in this research, a measurement error is added to the raw power vector to account for accuracy limitations in the hardware and modelling flaws.

2.4.2 Parameter Estimation. Although the assumptions made in Chapter 1 state that the transmission media is linear, isotropic and homogenous, the material constants used are only approximate. Perfect knowledge of these values is impossible so approximations are made. An error is added to each material constant to account for these imperfections.

2.4.3 Transmission/Reception Power. The received power vector magnitude is a function of transmission power and the media skin depth. The transmitters and receivers are hardware that cannot perfectly measure the power transmitted or received. This power measurement error is dependent largely on the equipment used and its specifications.

2.5 Nonlinear Least Squares Estimation

In this research, it is necessary to generate a state estimate utilizing the positioning methods previously outlined. However, these positioning methods involve solving highly nonlinear, over-determined systems of equations. In order to find a solution, a technique known as iterative least squares estimation will be used.

The objective of a *linear* least squares estimator is to find one solution among all possible solutions that minimizes the mean square difference between actual and generated observations [6]. The process of minimizing the sum of the squares of the observation errors is known as the the method of least squares. Due to the nonlinear nature of the positioning methods used in this research, linear corrections to a reference (nominal) position, $\hat{\mathbf{x}}$, must be made. These corrections, $\mathbf{\Delta x}$, are what the nonlinear least squares estimation technique is trying to estimate.

All of the measurements used in this research are available before the estimation process begins. Unlike a Kalman filter that updates the estimated states as new measurements come in, this estimation technique processes the measurements all at the same time, or in a batch. Each of the observations, 1 to n, are related to the states being estimated by:

$$z_i(t_i) = h(x(t_i), t_i) \tag{2.25}$$

where

z_i is the observation, or measurement, vector at time t_i

$h(x(t_i), t_i)$ is a nonlinear function that relates the measurements to the states

i is the index of the observations in the batch

In order estimate the state $x(t_i)$, the nonlinear $h(x(t_i), t_i)$ must be linearized to form the observation matrix $\mathbf{H}$:

$$\mathbf{H}_i = \frac{\partial h(x(t_i), t_i)}{\partial \hat{\mathbf{x}}} \tag{2.26}$$

18

where

$\mathbf{H}_i$ is the ith row of the observation matrix $\mathbf{H}$ corresponding to ith measurement

$\hat{\mathbf{x}}$ is the nominal position vector

Each iteration of the least squares estimation technique uses the residual (difference of the actual and calculated) observations, $\mathbf{\Delta p}$, to estimate the state corrections, $\mathbf{\Delta x}$:

$$\mathbf{\Delta x} = (\mathbf{H^T H})^{-1} \mathbf{H^T \Delta p} \tag{2.27}$$

The corrected state vector $\mathbf{x}$

$$\mathbf{x} = \hat{\mathbf{x}} + \Delta \mathbf{x} \tag{2.28}$$

is then used as the nominal position for subsequent iterations until the corrections, $\mathbf{\Delta x}$, fall below a predetermined threshold ϵ_{nom}. At that point, the final corrected state vector $\mathbf{x}$ is the least squares estimation solution.

2.6 Signals of Opportunity

Signals of opportunity are electromagnetic waves from known or unknown sources that are exploited for the purposes of navigation. They are generally uncontrolled and exist independently of the system in question. These can be naturally occurring signals or man-made. Some examples of man-made signals of opportunity include radio, television, and cell-phone signals. Naturally occurring signals of opportunity are generated from lightning strikes and earthquakes. In this research, naturally occurring signals of opportunity in the very-low frequency range will be utilized.

Lightning is the source of most naturally occurring VLF emissions on earth [2]. As lightning strikes the ground, a visible flash and a broadband pulse of radio waves are generated. These radio waves then propagate large distances, thousands of kilometers, by travelling in a natural waveguide created by the earth's surface and the ionosphere. As the radio waves travel through the waveguide, higher frequencies are

separated from lower frequencies due to delay dispersion. The wave guide has a natural low-frequency cutoff around 3kHz and allows frequencies above this to propagate.

The frequency range of interest for this research is just above the cutoff, 3kHz to 10kHz. This range is well above the 60 Hz power grid and below the Russian ALPHA 13 kHz navigation signals.

2.7 Conclusion

This chapter discussed the fundamental concepts pertinent to the research. First, a basic overview electromagnetic wave propagation was given. Elementary geometry was then reviewed as related to the following section on positioning. Next, typical errors found in this research were discussed. Nonlinear Least squares estimation was then addressed as it was used in this research. Finally, signals of opportunity rounded out the chapter. In Chapter 3, these concepts are be brought to bear as positioning algorithms for the simulations are developed.

III.   Methodology

This chapter explains in detail the algorithms used for this research based on the concepts from the previous chapter. Each simulation was implemented in MATLAB® and is described in detail, starting with the parameters used, truth model and measurement generation, and the method used to calculate a position solution with an associated standard deviation. The second section covers a simulation of the first sub-surface navigation scheme using above ground transmitters and a below ground mobile receiver. This chapter also describes the software simulation of a VLF data collection system that exploits signals of opportunity to formulate a position solution. Finally, a brief overview of the performance analysis used to quantify the results is given.

3.1   Reference Coordinate System

In this research, the reference coordinate system is the local level frame expressed in cartesian coordinates. This was done for simplicity and relative positioning within a given operational area. It is straight-forward to transform the local level frame into any frame of reference that is needed for actual implementation. The simulations are all expressed in meters from the origin $(0, 0, 0)$.

3.2   Simulation of the Transmitter/Receiver Scheme

This section covers the simulation created in MATLAB® for the first sub-surface navigation scheme shown in Figure 3.1 using above ground transmitter beacons with a below ground mobile receiver. A 3-dimensional position solution is found. Figure 3.2 shows the block diagram for the transmitter/receiver scheme simulation.

3.2.1 Parameters.   The parameters block is used to initialize the simulation with user defined variables as well as universal constants such as the speed-of-light. The following user defined variables can be set to achieve a desired test:
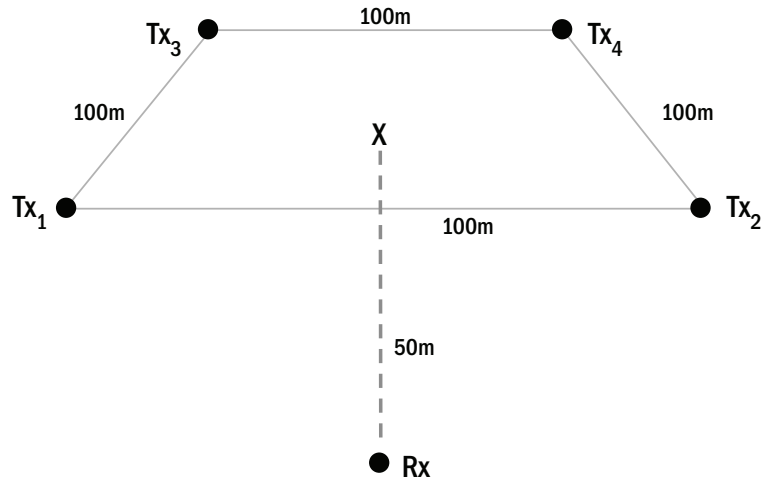
Figure 3.1:   Diagram of the transmitter/receiver scheme.
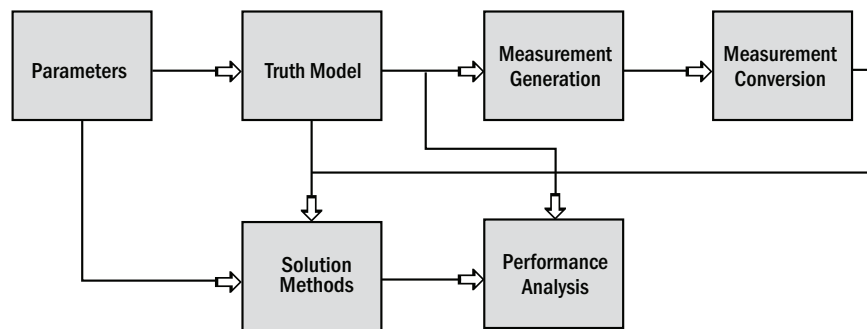
Figure 3.2:   Transmitter/receiver scheme simulation block diagram.

- Number of Transmitters: the number of transmitters used for the simulation (minimum of three)

- Location of Transmitters: the location for each transmitter in the local frame (m)

- Transmission Frequency: broadcast frequency of each transmitter (Hz)

- Transmission Power: broadcast power of each transmitter (W)

- Mobile Minimum Power: the minimum power the mobile receiver can detect and still produce a field vector (W)

- Nominal Position: the nominal position used for the least squares iteration; the z-axis coordinate must be negative to iterate to a negative z-axis position solution (m)

- Nominal Iteration Threshold: the threshold, ϵ_{nom}, at which the least squares iteration stops

- Material Constants: the conductivity, σ, the permeability, μ, and the permittivity, ϵ, for the simple media used for this simulation.

- Error Standard Deviations: the standard deviation of the error sources that can be introduced into the simulation

  - Raw Field Vector: three axis error standard deviation of the mobile receivers measurements $(\delta x, \delta y, \delta z)$

  - Material Constants: each material constant is given an associated error to model uncertainties in the constants $(\delta \sigma, \delta \mu, \delta \epsilon)$

  - Transmission Power: the transmission power is also given an associated error due to transmitter hardware inaccuracies (δP)

  - Transmitter Location: error associated with the transmitter's location due to GPS or other location errors

3.2.2   Truth Model.   The truth model block receives its inputs from the parameters block to serve as a reference or truth for the simulation. The true error-free position of the mobile receiver is set as well as the true position of the transmitters. All position error calculations use these reference positions to determine the inaccuracy of the position solution.

3.2.3   Generated Measurements.   The measurements used by the simulation are created in the generated measurements block. The measurements generated are direct EM field vector power measurements along each axis referred to as raw power vector and Type III measurements. This is done by using: 1) the simplified skin depth formula from (2.10),

$$\delta_{SD} = \frac{1}{\sqrt{\pi f \mu \sigma}} \tag{3.1}$$

where

   f is the transmission frequency

   μ is the permeability

   σ is the conductivity

2) a normalized unit pointing vector from the mobile receiver to each transmitter,

$$\frac{\mathbf{x_i} - \mathbf{x_{truth}}}{\|\mathbf{x_i} - \mathbf{x_{truth}}\|} \tag{3.2}$$

where

   $\mathbf{x_i}$ is the position of the ith transmitter

   $\mathbf{x_{truth}}$ is the true position of the mobile

and 3) the transmission power of each transmitter P_i. The material constants error sources as specified in the parameters block are added into the skin depth as follows:

$$\delta_{SDE} = \frac{1}{\sqrt{\pi f (\mu + \delta \mu)(\sigma + \delta \sigma)}} \tag{3.3}$$

The final measurements are then calculated with the transmission power and received field vector errors [reference]:

$$\mathbf{z_i} = \left(\frac{\mathbf{x_i} - \mathbf{x_{truth}}}{\|\mathbf{x_i} - \mathbf{x_{truth}}\|}\right)(P_i + \delta P)e^{-\frac{\|\mathbf{x_i} - \mathbf{x_{truth}}\|}{\delta_{SDE}}} + \delta\mathbf{z} \tag{3.4}$$

where

$\mathbf{z_i}$ is the ith vector measurement

$\delta\mathbf{z}$ is the error vector with standard deviation of $(\delta x, \delta y, \delta z)$ for the received field

3.2.4   Converted Measurements.   For two of the solution methods outlined in the next section to work, the measurements generated by the previous block must be converted to a useful format. The converted measurements block takes the raw power vector measurements from each transmitter from the previous block and calculates an approximated measurement length between the mobile receiver and the associated transmitter and also creates a difference angle between two transmitter vectors with the mobile receiver at the apex.

The first conversion takes the raw measurements from the generated measurement block and attempts to calculate a range (m), or length (Type I measurement), from the mobile receiver to each corresponding transmitter. The entered material constants in the parameter block are used as approximations for the skin depth formula. The assumed transmission power is then used with the above skin depth to calculate the distance the EM wave must have travelled to generate that particular field strength as follows:

$$l_i = \left|\ln\left(\frac{P_i}{\|\mathbf{z_i}\|}\right)\delta_{SD}\right| \tag{3.5}$$

where

l_i is the ith measurement of length

The second conversion is to find a difference angle (Type II measurement) between two measurement vectors associated with a pair of transmitters by means of the

Law of Cosines. Each pair of transmitters generates one difference angle measurement by:

$$\theta_{ij} = \arccos\left(\frac{\mathbf{z_i} \cdot \mathbf{z_j}}{\|\mathbf{z_i}\|\|\mathbf{z_j}\|}\right) \tag{3.6}$$

where

θ_{ij} is the ijth measurement of a difference angle between a pair of transmitters i and j

3.2.5   Solution Methods.   The position solution block uses two separate solution methods to create a position, a least squares iteration technique and a line fit. The converted measurements of length, l_i, and difference angle, θ_{ij}, as well as the raw power vector measurements, z_i, are used in the algorithms presented here.

3.2.5.1   Nonlinear Least Squares Estimation.   To solve for a position solution, a nominal position, $\hat{\mathbf{x}}$, is entered in the simulation. A least squares technique is iterated until the corrections to the nominal fall below a threshold ϵ_{nom}. As shown in (2.27), $\mathbf{\Delta x}$, $\mathbf{H}$, and $\mathbf{\Delta p}$ must be found.

When using the first measurement of length to find a position solution, the observation matrix $\mathbf{H}$ is formed using the partial derivative with respect to the nominal, $\hat{\mathbf{x}}$, of the following length measurement equation:

$$l_i = \sqrt{(x_{mob} - x_i)^2 + (y_{mob} - y_i)^2 + (z_{mob} - z_i)^2} \tag{3.7}$$

where

l_i is the distance from the nominal position to the ith transmitter

Then from (2.27), the correction vector $\mathbf{\Delta x}$ is solved using:

$$\mathbf{\Delta x} = (\mathbf{H^T H})^{-1}\mathbf{H^T \Delta p} \tag{3.8}$$

where

$$\Delta\mathbf{x} = \begin{pmatrix} \Delta x \\ \Delta y \\ \Delta z \end{pmatrix} \qquad \mathbf{H} = \begin{pmatrix} \frac{\hat{x}-x_1}{r_1} & \frac{\hat{y}-y_1}{r_1} & \frac{\hat{z}-z_1}{r_1} \\ \frac{\hat{x}-x_2}{r_2} & \frac{\hat{y}-y_2}{r_2} & \frac{\hat{z}-z_2}{r_2} \\ . & . & . \\ \frac{\hat{x}-x_n}{r_n} & \frac{\hat{y}-y_n}{r_n} & \frac{\hat{z}-z_n}{r_n} \end{pmatrix} \qquad \Delta\mathbf{p} = \begin{pmatrix} l^1_{meas} - l_1|_{\hat{\mathbf{x}}} \\ l^2_{meas} - l_2|_{\hat{\mathbf{x}}} \\ . \\ l^n_{meas} - l_n|_{\hat{\mathbf{x}}} \end{pmatrix}$$

$$r_i = \sqrt{(\hat{x} - x_i)^2 + (\hat{y} - y_i)^2 + (\hat{z} - z_i)^2}$$

l^i_{meas} is the ith converted length measurement

The estimated state is then corrected by $\Delta\mathbf{x}$ using:

$$\hat{\mathbf{x}} = \hat{\mathbf{x}} + \Delta\mathbf{x} \tag{3.9}$$

The nominal position is updated until $\Delta\mathbf{x}$ falls below the iteration threshold, ϵ_{nom}, specified in the parameters block. Once the iterations are complete, the final position solution is:

$$\mathbf{x_{mob}} = \hat{\mathbf{x}} \tag{3.10}$$

For the difference angle measurement, $\Delta\mathbf{x}$, $\mathbf{H}$, and $\Delta\mathbf{p}$ are formed in a similar manner as the length measurement. First, the observation matrix $\mathbf{H}$ is formed using the partial derivative with respect to the nominal, $\hat{\mathbf{x}}$, of the difference angle measurement equation:

$$\theta_{ij} = \arccos\left(\frac{(\mathbf{x_i} - \hat{\mathbf{x}}) \cdot (\mathbf{x_j} - \hat{\mathbf{x}})}{\|(\mathbf{x_i} - \hat{\mathbf{x}})\| \|(\mathbf{x_j} - \hat{\mathbf{x}})\|}\right) \tag{3.11}$$

where

θ_{ij} is the ijth measurement of a difference angle between a pair of transmitters i and j

Again, the correction vector $\boldsymbol{\Delta}\mathbf{x}$ is solved using:

$$\boldsymbol{\Delta}\mathbf{x} = (\mathbf{H^T H})^{-1}\mathbf{H^T}\boldsymbol{\Delta}\mathbf{p} \tag{3.12}$$

where

$$\boldsymbol{\Delta}\mathbf{x} = \begin{pmatrix} \boldsymbol{\Delta}x \\ \boldsymbol{\Delta}y \\ \boldsymbol{\Delta}z \end{pmatrix} \qquad \mathbf{H} = \begin{pmatrix} h1_{12} & h2_{12} & h3_{12} \\ h1_{13} & h2_{13} & h3_{13} \\ . & . & . \\ h1_{mn} & h2_{mn} & h3_{mn} \end{pmatrix} \qquad \boldsymbol{\Delta}\mathbf{p} = \begin{pmatrix} \theta_{meas}^{12} - \theta_{12}|_{\hat{\mathbf{x}}} \\ \theta_{meas}^{13} - \theta_{13}|_{\hat{\mathbf{x}}} \\ . \\ \theta_{meas}^{mn} - \theta_{mn}|_{\hat{\mathbf{x}}} \end{pmatrix}$$

$$h1_{ij} = \frac{(-x_i + 2\hat{x} - x_j) + \frac{c}{\sqrt{a}}(x_i - \hat{x}) + \frac{c}{\sqrt{b}}(x_j - \hat{x})}{\sqrt{ab - c^2}}$$

$$h2_{ij} = \frac{(-y_i + 2\hat{y} - y_j) + \frac{c}{\sqrt{a}}(y_i - \hat{y}) + \frac{c}{\sqrt{b}}(y_j - \hat{y})}{\sqrt{ab - c^2}}$$

$$h3_{ij} = \frac{(-z_i + 2\hat{z} - z_j) + \frac{c}{\sqrt{a}}(z_i - \hat{z}) + \frac{c}{\sqrt{b}}(z_j - \hat{z})}{\sqrt{ab - c^2}}$$

$$a = (x_i - \hat{x})^2 + (y_i - \hat{y})^2 + (z_i - \hat{z})^2$$

$$b = (x_j - \hat{x})^2 + (y_j - \hat{y})^2 + (z_j - \hat{z})^2$$

$$c = (x_i - \hat{x})(x_j - \hat{x}) + (y_i - \hat{y})(y_j - \hat{y}) + (z_i - \hat{z})(z_j - \hat{z})$$

θ_{meas}^{ij} is the ijth converted angle difference measurement

$$\hat{\mathbf{x}} = \hat{\mathbf{x}} + \boldsymbol{\Delta}\mathbf{x} \tag{3.13}$$

As above, the nominal position is updated until $\boldsymbol{\Delta}\mathbf{x}$ falls below the iteration threshold, ϵ_{nom}, specified in the parameters block. Once the iterations are complete, the final position solution is:

$$\mathbf{x_{mob}} = \hat{\mathbf{x}} \tag{3.14}$$

3.2.5.2 Line Fit. The actual field vector measurements themselves can be used directly by means of a line fit if an inertial navigation system (INS) is onboard the mobile receiver. The INS is needed to ensure the vectors are given in the
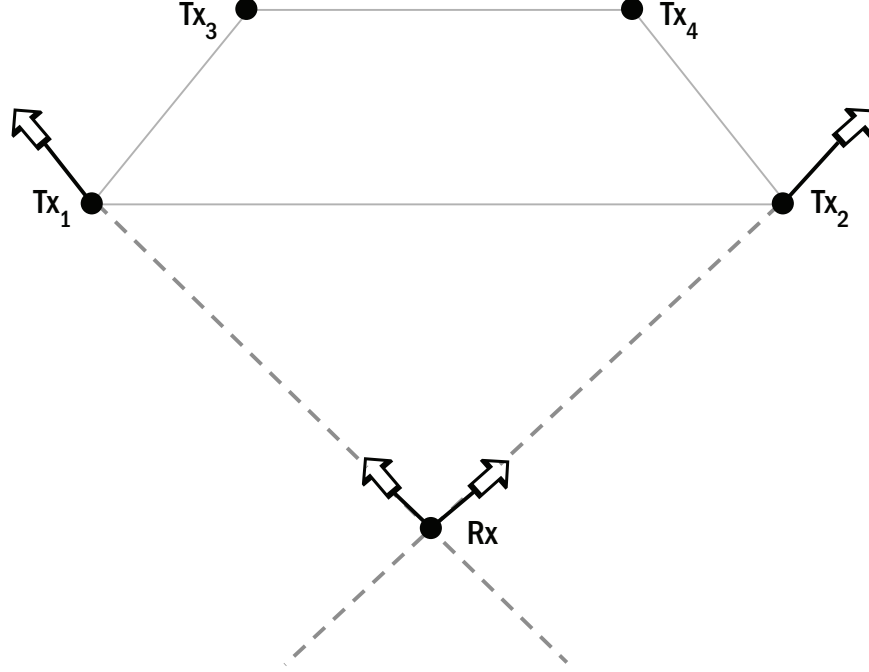
Figure 3.3:   Linear line fit with the measurement vector superimposed onto the transmitter.

local level frame. If the yaw, pitch, and roll of the mobile receiver is known, then the measurements are rotated using a standard direction cosine matrix.

After the measurements in the local level frame are known, the rotated measurement vector can be superimposed onto the corresponding transmitter that created the measurement. A line can then be extended from the transmitter into the negative z direction as shown in Figure 3.3. A second measurement vector creates an additional line and the intersection can be found by solving the following equations simultaneously by method of substitution [reference]:

$$\mathbf{x_{mob}} = \mathbf{x_i} + \mathbf{z_i}t_1 \tag{3.15}$$

$$\mathbf{x_{mob}} = \mathbf{x_j} + \mathbf{z_j}t_2 \tag{3.16}$$

where

$\mathbf{x_{mob}}$ is the intersection point

$\mathbf{x_i}$ is the ith transmitter position
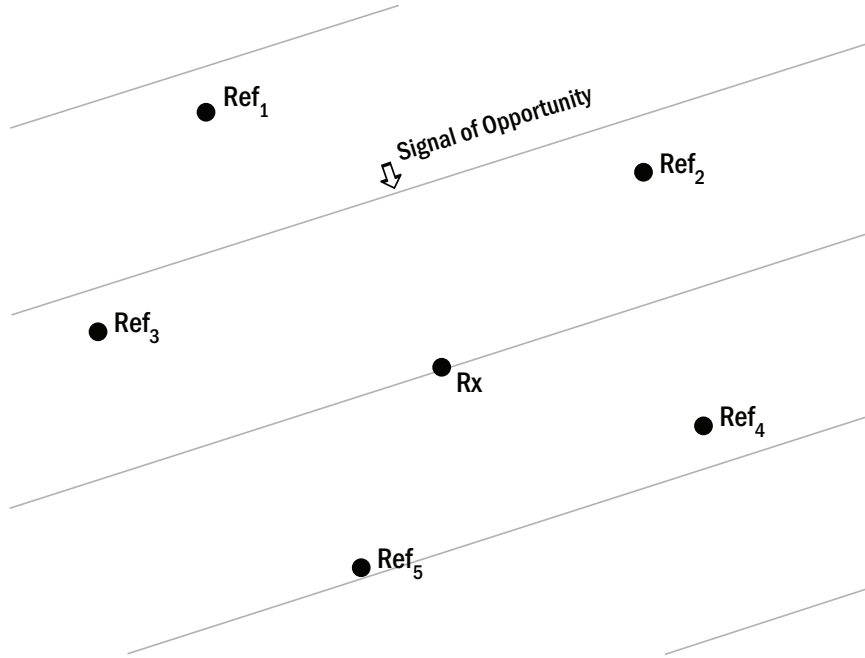
Figure 3.4:   Diagram of the VLF Data Collection System.

$\mathbf{x_j}$ is the jth transmitter position

$\mathbf{z_i}$ is the ith field vector measurement associated with the ith transmitter

$\mathbf{z_j}$ is the jth field vector measurement associated with the jth transmitter

t_1 and t_2 are the independent variables that designate where on the lines the point $\mathbf{x_{mob}}$ lies

This intersection point is the position solution of the mobile receiver. If additional measurements are received, an average solution of all solution pairs created is used.

3.3   Design of the Very-Low Frequency Data Collection System

The previous simulation dealt with placing multiple transmitters above ground with a single mobile receiver below ground. The next approach uses multiple receivers above ground as well as a single mobile receiver below ground to 'listen' for signals of opportunity as shown in Figure 3.4. The signals from each receiver are correlated with each other to form time differences of arrival between all of the receivers in the network. An important distinction to be made is that this scheme solves for a 2-
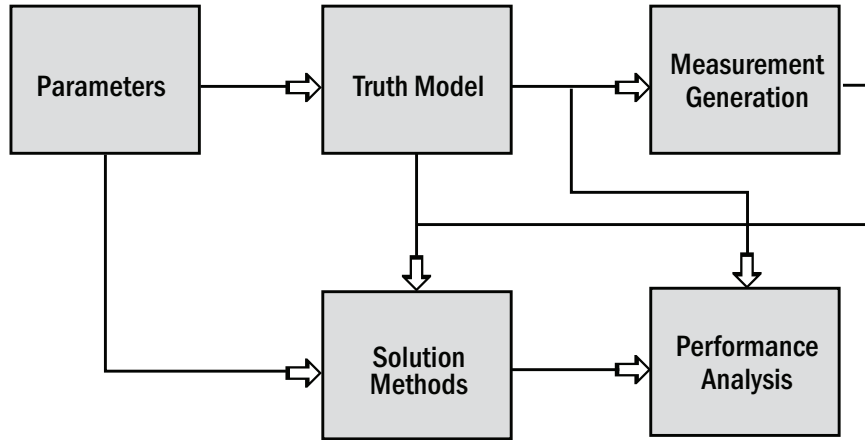
Figure 3.5:   VLF Data Collection System simulation block diagram.

dimensional position in x and y as well as the clock error of the mobile receiver. For the purposes of this simulation, measurements come after correlation is completed, (i.e., in time-difference-of-arrival format). The following sections will explain how this system will solve for a position solution. Figure 3.5 shows the block diagram for the VLF data collection system simulation.

3.3.1 Parameters.   As with the simulation in the previous section, the parameters block allows the user to define input variables as well as universal constants. The following parameters are used in this simulation:

- Number of Reference Receivers: defines the number of reference receivers used for the simulation with a minimum of four

- Location of Reference Receivers: defines the location for each reference receiver of the network in the local frame (m)

- Nominal Solution: defines the nominal solution used for the least squares iteration; the magnitude of the slope, $\hat{m}$, and y-intercept of the line, $\hat{b}$, are initialized in the nominal

- Slope of Incoming Signal: defines the slope of the line for incoming signals

31
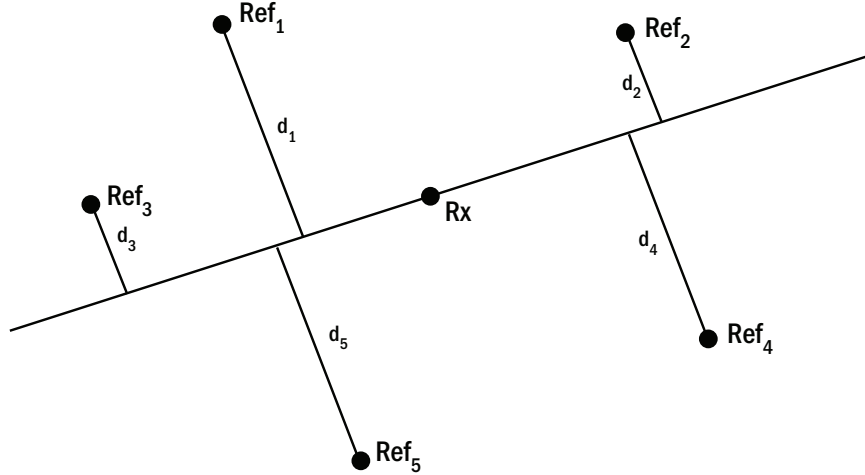
Figure 3.6:   Perpendicular offsets to a line.

- Nominal Iteration Threshold: defines the threshold, ϵ_{nom}, at which the least squares iteration stops

- Error Standard deviation of Received Time: each TDOA measurement has a random error added, δt (sec)

- Reference Receiver Location: error associated with the reference receiver's location due to GPS or other location errors

3.3.2   Truth Model.   The truth model block receives input from the parameters block to serve as a reference or truth for the simulation. The true error free position of the mobile receiver and clock error are set as well as the true position of the reference receivers. All position error calculations use these reference positions to determine the inaccuracy of the position solution.

3.3.3   Generated Measurements.   The measurements used by the simulation are created in the generated measurements block. These measurements come in the form of a TDOA between each of the reference receivers and the mobile receiver. They are formed by use of perpendicular offsets to a line as shown in Figure 3.6. A line is formed with the indicated slope from the parameters block that goes through the mobile truth position. Then the distance d_i each reference receiver at location

32

(x_i, y_i) is away from the line with slope m and y-intercept b is calculated using the perpendicular offset formula:

$$d_i = \frac{y_i - (mx_i + b)}{\sqrt{1 + m^2}} \tag{3.17}$$

The distance in meters is then divided by the speed-of-light in free space c to convert to a time in seconds. A random noise δt is induced on the measurement to simulate atmospheric and other effects. The final measurement is of the form:

$$z_i = \frac{d_i}{c} + \delta t \tag{3.18}$$

3.3.4 Solution Method. The solution method for the VLF data collection system uses an iterative least square approach just as the transmitter/receiver scheme used. However, it is broken down into two parts. Part 1 uses the TDOA measurements and solves for a line in slope-intercept form that is parallel to the wavefront of each incoming signal. Part 2 uses these lines to solve for a position solution using weighted least squares.

As with the previous simulation, a nonlinear least squares technique is used to solve for each line. However, the nominal solution cannot be completely assigned beforehand. The measurements that are brought in to the solution block are ambiguous in that they can iterate to a positive or negative slope of a solution line and only one of them can be the correct solution. In order to solve for this ambiguity, an approximate slope, $\tilde{m}$, must be found to initialize the nominal slope in the proper direction.

Since the measurements are signed, they can be ordered from most negative to most positive. The most negative measurement is set to be the first incoming measurement continuing in order to the most positive as the last measurement. Using

(3.22) for the first two measurements:

$$d_1 = \frac{y_1 - (\tilde{m}x_1 + b)}{\sqrt{1 + \tilde{m}^2}} \tag{3.19}$$

$$d_2 = \frac{y_2 - (\tilde{m}x_2 + b)}{\sqrt{1 + \tilde{m}^2}} \tag{3.20}$$

where

d_1 and d_2 are the first two measurements

(x_1, y_1) is the known position of the first receiver

(x_2, y_2) is the known position of the second receiver

and subtracting d_2 from d_1 and solving for the approximate slope $\tilde{m}$ yields:

$$\tilde{m}^2 + \left[\frac{2(x_2 - x_1)(y_1 - y_2)}{(x_2 - x_1)^2 - (d_1 - d_2)^2}\right]\tilde{m} + \frac{(y_1 - y_2)^2 - (d_1 - d_2)^2}{(x_2 - x_1)^2 - (d_1 - d_2)^2} = 0 \tag{3.21}$$

Since (3.21) is in quadratic form, $\tilde{m}$ has two solutions and must narrowed even further. Equation 3.19 can be solved again for the second and third measurements which creates an additional solution pair for $\tilde{m}$. One of the solutions from this pair will match closely with one of the solutions from the first pair. The sign of this matched solution will be the nominal slope sign.

Now that the nominal can be fully initialized, the observation matrix $\mathbf{H}$ is formed with n measurements using the partial derivative with respect to the nominal, $(\hat{b}, \hat{m})$, of the following TDOA measurement equation:

$$d_i = \frac{|y_i - (\hat{m}x_i + \hat{b})|}{\sqrt{1 + \hat{m}^2}} \tag{3.22}$$

Then from (2.27), the correction vector $\mathbf{\Delta x}$ is solved using:

$$\mathbf{\Delta x} = (\mathbf{H^T H})^{-1}\mathbf{H^T \Delta p} \tag{3.23}$$

where

34

$$\mathbf{\Delta x} = \begin{pmatrix} \mathbf{\Delta}b \\ \mathbf{\Delta}m \end{pmatrix} \qquad \mathbf{H} = \begin{pmatrix} h1_1 & h2_1 \\ h1_2 & h2_2 \\ . & . \\ h1_n & h2_n \end{pmatrix} \qquad \mathbf{\Delta p} = \begin{pmatrix} d^1_{meas} - d_1|_{\hat{\mathbf{x}}} \\ d^2_{meas} - d_2|_{\hat{\mathbf{x}}} \\ . \\ d^n_{meas} - d_n|_{\hat{\mathbf{x}}} \end{pmatrix}$$

$h1_i = -\frac{sgn(a_i)}{\sqrt{1+\hat{m}^2}}$

$h2_i = -sgn(a_i)(\frac{x_i}{\sqrt{1+\hat{m}^2}} + \frac{a_i\hat{m}}{1+\hat{m}^2})$

$a_i = \frac{y_i - (\hat{m}x_i + \hat{b})}{\sqrt{1+\hat{m}^2}}$

d^i_{meas} is the ith TDOA measurement

$$\hat{\mathbf{x}} = \hat{\mathbf{x}} + \mathbf{\Delta x} \tag{3.24}$$

The nominal solution of the line is updated until $\mathbf{\Delta x}$ falls below the iteration threshold, ϵ_{nom}, specified in the parameters block. Once the iterations are complete, the solution for Part 1 is $\hat{\mathbf{x}}$.

To solve for the mobile receiver's position in Part 2, the n solutions from Part 1 are used in a weighted least squares technique. Each solution corresponds to a line of the form:

$$y_{mob} = m_i x_{mob} + b_i \tag{3.25}$$

where

(x_{mob}, y_{mob}) is the mobile receiver's position estimate

m_i is the ith solution slope from Part 1

b_i is the ith solution y-intercept from Part 1

Accounting for n solution lines, (3.25) can be written in matrix form as:

$$\mathbf{A}\mathbf{x_{mob}} = \mathbf{B} \tag{3.26}$$

35

where

$$\mathbf{A} = \begin{pmatrix} -m_1 & 1 \\ -m_2 & 1 \\ \cdot & \cdot \\ -m_n & 1 \end{pmatrix} \qquad \mathbf{x_{mob}} = \begin{pmatrix} x_{mob} \\ y_{mob} \end{pmatrix} \qquad \mathbf{B} = \begin{pmatrix} b_1 \\ b_2 \\ \cdot \\ b_n \end{pmatrix}$$

Using a weighted least squares approach, the mobile receiver's position, $\mathbf{x_{mob}}$, can be solved:

$$\mathbf{x_{mob}} = (\mathbf{A^T C A})^{-1} \mathbf{A^T C B} \tag{3.27}$$

where

$\mathbf{C}$ is an $n \times n$ diagonal weighting matrix described below

The weighting matrix, $\mathbf{C}$, is an ad-hoc way of accounting for the inaccuracies of the slope-intercept solution in Part 1. It has as it's diagonal elements a value corresponding to each solution line's slope. As the slope of a line grew larger, the associated error of the solution line also grew. In an attempt to account for this error, the line's standard deviation matrix $\mathbf{H^T H}$ was observed for each run. The diagonal entry corresponding to large slopes was indeed very large in comparison to those entries corresponding to slopes from 0 to 1. The inverse of these entries was then used as the diagonal elements in the weighting matrix to put less weight on those lines with large slopes. The weighting matrix presented here is only one way to address the issue. There may be better ways to derive the weighting matrix.

3.4 Performance Analysis

The purpose of the performance analysis block for both simulations is to compare the calculated mobile receiver position from the solution method block with the truth position designated in the truth model block. The calculated mobile receiver

position, $\mathbf{x_{mob}}$, is related to the truth position, $\mathbf{x_{truth}}$, by:

$$\delta\mathbf{x_{error}} = \mathbf{x_{mob}} - \mathbf{x_{truth}} \tag{3.28}$$

Using a Monte Carlo analysis, the standard deviation of $\delta\mathbf{x_{error}}$ is found over 1000 runs.

The transmitter/receiver scheme from Section 3.2 also computes a contour map of the transmitter coverage area. This coverage area shows where at least three measurements can be received in order to generate a position solution. If the mobile receiver moves outside the given contour, then a position solution cannot be found.

3.5 *Random Number Seed*

For error generation, this simulation uses MATLAB®'s randn() function which creates a random normally distributed Gaussian number. The capability to generate the same sequence of random numbers for each run is needed so that the only thing that changes between runs is the variable of interest such as the position of the transmitters or truth location of the receiver. This is done by manually setting the 'seed, or beginning point, in the random number generator so that it starts from the same place each time.

3.6 *Summary*

This chapter presented two simulations for use with sub-surface navigation. The simulations were broken down into block descriptions and it was shown how each block interacts with adjacent blocks. A performance analysis for the simulations was given and the random number seed concept was explained. The next chapter explores various trade studies to analyze each simulations performance.

IV. Results and Analysis

This chapter presents the results and detailed analysis of the simulations used in this research. Both simulation's results will be described separately in their respective sections. First a baseline result is given and used to compare to the results of the subsequent trade studies. Each trade study starts with an explanation of its purpose and how it was implemented. An analysis of the trade study's results is then provided. A 1000 run Monte Carlo analysis was used to evaluate all simulations.

4.1 Transmitter/Receiver Scheme

This section details the results for the first of the two simulations, the transmitter/receiver scheme. The trade studies utilized the baseline parameters but certain parameters are varied to achieve the desired outcome. The trade studies include varying the number and positions of the transmitters, varying the position of the mobile receiver, and varying some of the error sources involved in the simulation.

A 'zero-error check' was performed on the simulation for which all errors were set to zero. This is to ensure that the simulated algorithms are working as intended. When this was done, a position solution converged with an error less than 10^{-12} m from the truth in all three axes.

4.1.1 Baseline Results.   The baseline results establish reference data to evaluate the subsequent trade studies. Given the assumptions made in Chapter 1, the baseline shows general performance of the transmitter/receiver scheme. The primary goal of the research is to solve for a position solution and associated standard deviation based on certain parameters. The parameters used for the baseline simulation are given in Table 4.1. The four transmitters are arrayed in a square formation separated by 100 m each with one transmitter at the origin. Ground-level is considered to be at zero depth while sub-surface is defined as any negative depth. All four transmitters are positioned at ground-level.

Table 4.1: Navigation Scheme 1: Baseline parameters.

Parameter	Value
Number of Transmitters	4
Transmission Frequency	10 kHz
Transmission Power	100 watts
Mobile Minimum Power	40 watts
Nominal Position	$(10, 10, -15)$
Permeability, μ	$4\pi \times 10^{-7}$
Conductivity, σ	10^{-3}
Raw Power Vector Error x-axis, δx_p	0.5 watts
Raw Power Vector Error y-axis, δy_p	0.5 watts
Raw Power Vector Error z-axis, δz_p	0.5 watts
Permeability Error, $\delta\mu$	0
Conductivity Error, $\delta\sigma$	0
Transmission Power Error, δP	0 watts
Transmitter Location Error x-axis, δx_L	0 meters
Transmitter Location Error y-axis, δy_L	0 meters
Transmitter Location Error z-axis, δz_L	0 meters

For the baseline simulation, the mobile receiver is positioned at the coordinates $(50, 30, -50)$. The received raw power vector errors were added to the raw power vector measurements (Type III) for each axis. The same raw power vector measurements were then converted into a length (Type I) and a difference angle (Type II). The three measurement types were used separately to solve for a position solution, as described in Sections 3.2.3 and 3.2.4. All results given will reflect the horizontal and vertical accuracy of each measurement type used.

Table 4.2 shows the results of the baseline simulation for each measurement type. The standard deviation of the position error (m) taken over 1000 runs is given for each axis. Figure 4.1 shows the contour map of the coverage area. The Type III, or raw field vector, measurements have the best horizontal error standard deviation but requires the use of an Inertial Navigation System (INS). Without an INS, Type II, or difference angle measurements, resolve a better horizontal position solution than the Type I, or length, measurements by 20% and vertical by 150%.

39
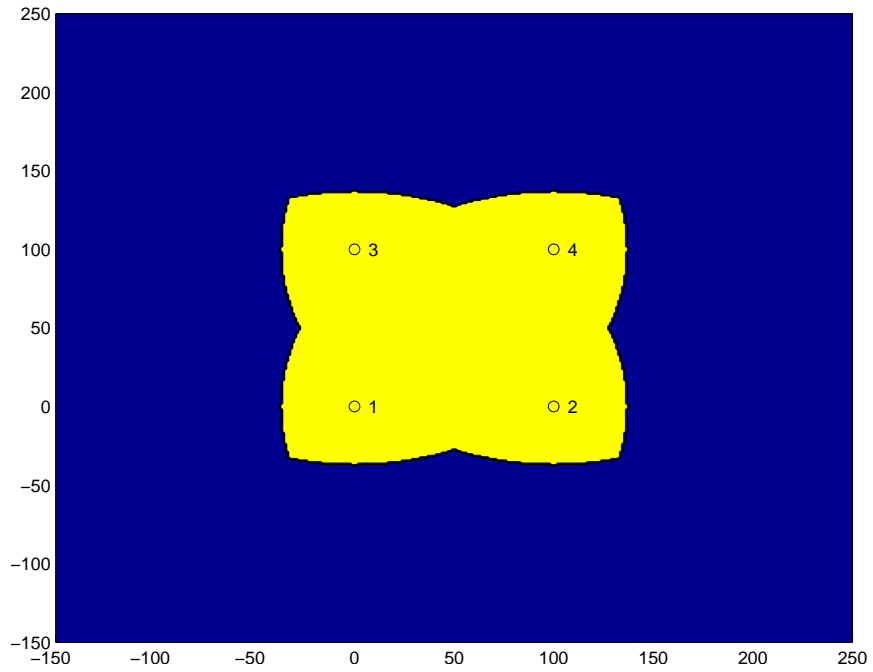
Figure 4.1:   Navigation Scheme 1: Baseline contour plot of coverage area.

Table 4.2:   Navigation Scheme 1: Baseline position error standard deviation.

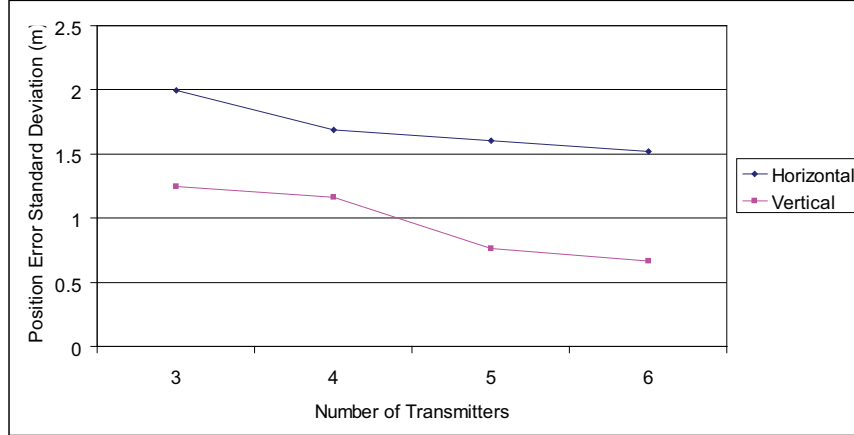| Measurement Type	Horizontal (m)	Vertical (m)
Length (1)	1.685	1.166
Difference Angle (2)	1.351	0.466
Raw Power Vector (3)	0.639	0.483

40

Figure 4.2:   Navigation Scheme 1: Effect of number of transmitters on measurement Type I (length) accuracy.

4.1.2 Trade Study 1: Vary Number of Transmitters.   The purpose of this trade study is to see how the standard deviation of the position error changes due to a different number of transmitters. The baseline uses four transmitters arrayed in a square formation. This trade study uses three, five, and six transmitters to solve for a position. No other parameter changes are made.

The transmitters for each trade study are arrayed in a formation similar to the polygon with the number of sides equal to the number of transmitters, i.e., a triangle for three transmitters and a pentagon for five, with a centroid at approximately $(50, 30, 0)$. Again, 1000 runs for each formation was used to create a position error standard deviation. Figures 4.2-4.4 give the results for each of the formations. A contour plot for each of the formations is also included in Figures 4.5-4.7.

The data shows that as the number of transmitters increases, both horizontal and vertical error standard deviations decrease. This is due to more measurements becoming available to create a position solution. As each measurement is added, more information about the position becomes known and is reflected in a decreased error standard deviation. The contour plots created for this trade study show that as the number of transmitters increase, the coverage area also increases.

41

Figure 4.3:   Navigation Scheme 1: Effect of number of trans-
mitters on measurement Type II (difference angle) accuracy.
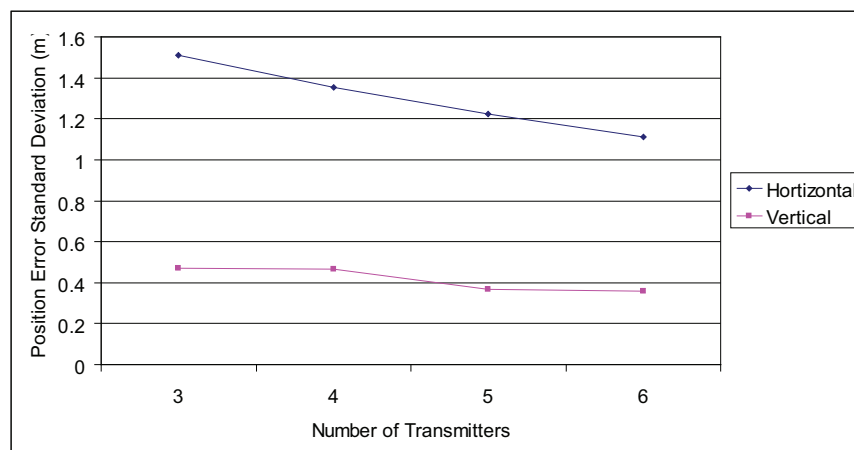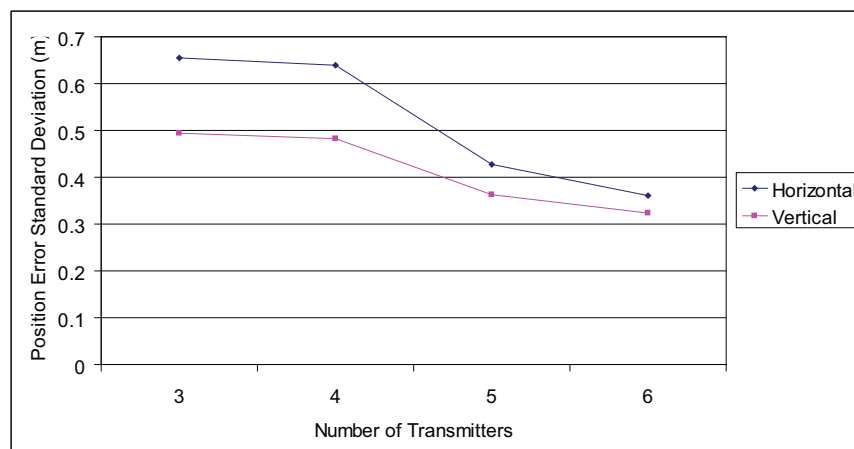

Figure 4.4:   Navigation Scheme 1: Effect of number of trans-
mitters on measurement Type III (received power vector) accu-
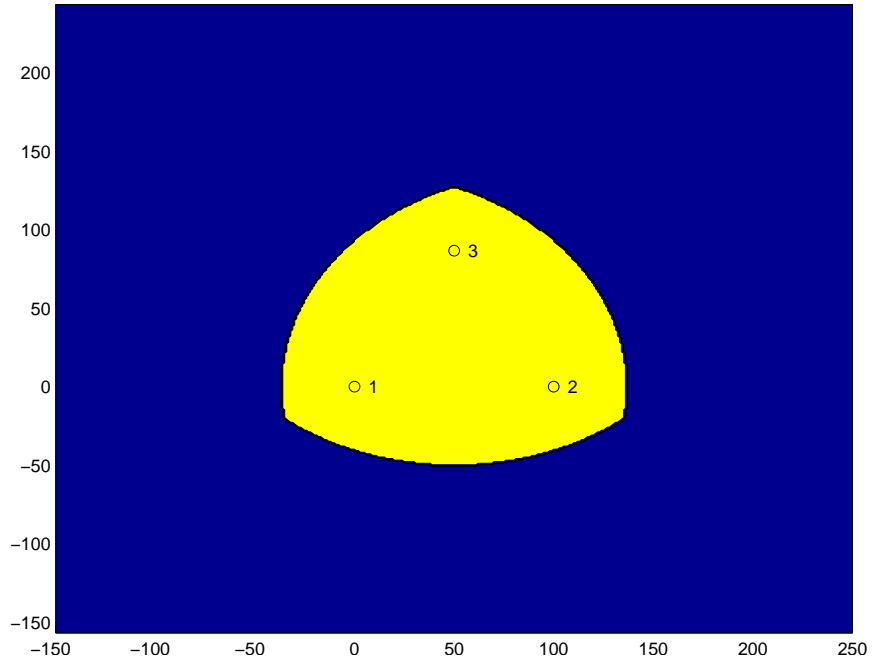racy.

Figure 4.5:   Navigation Scheme 1: Three transmitter setup contour plot of coverage area.
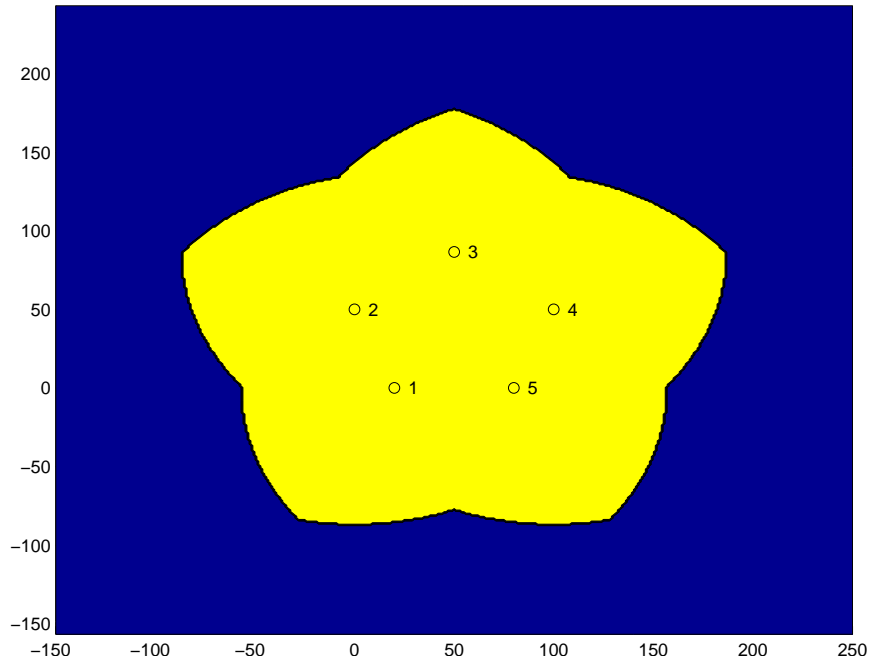
Figure 4.6:   Navigation Scheme 1: Five transmitter setup contour plot of coverage area.
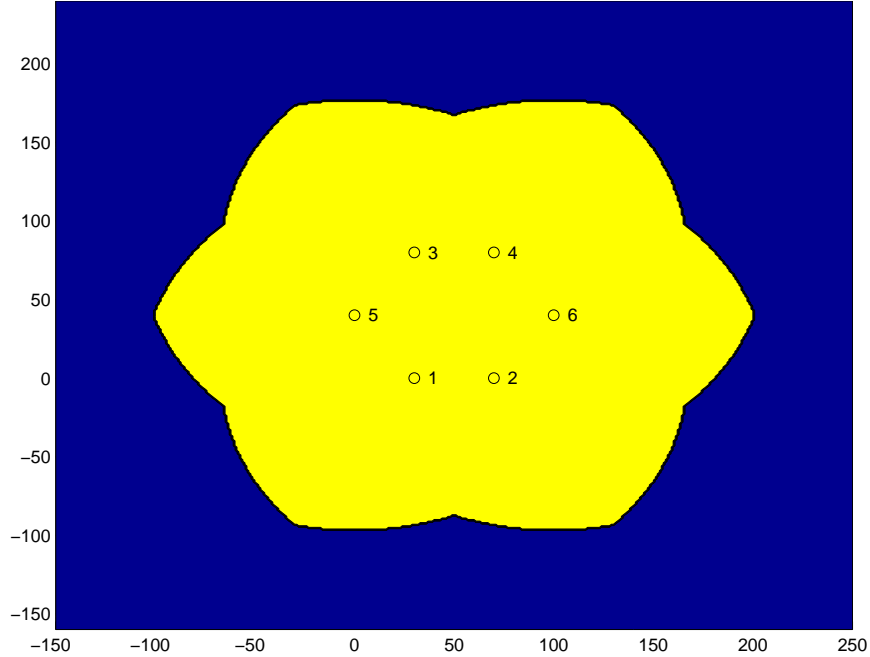
Figure 4.7: Navigation Scheme 1: Six transmitter setup contour plot of coverage area.

4.1.3 Trade Study 2: Vary Locations of Transmitters. It is useful to quantify the errors that GPS may introduce to the system. In the baseline simulation, perfect knowledge of the locations of the transmitters was assumed. For this trade study, an error is added to the location of each transmitter to simulate the inaccuracies of a GPS position. The true locations of the transmitters are assumed to be the same as the baseline which are used to create the measurements. The algorithm then uses the estimated location of the transmitters to derive the mobile position solution. Table 4.3 shows the horizontal and vertical standard deviation of transmitter locations used for each test. All other parameters are left unchanged. Figures 4.8-4.10 show the results for this trade study.

The results show that as the location error standard deviation increases linearly, the position errors increase exponentially. As the data follows its current trend, Type I would become the best solution method for a horizontal position for varying locations of the transmitters. Type II would have the best overall accuracy in the vertical direction.

44

Table 4.3: Navigation Scheme 1: Error standard deviation for transmitter locations used for Trade Study 2.

Test	δx_L(m)	δy_L(m)	δz_L(m)
1	0	0	0
2	0.5	0.5	0.5
3	1	1	1
4	1.5	1.5	1.5
5	2	2	2

Figure 4.8: Navigation Scheme 1: Effect of location of transmitters on measurement Type I (length) accuracy.

Figure 4.9: Navigation Scheme 1: Effect of location of transmitters on measurement Type II (difference angle) accuracy.

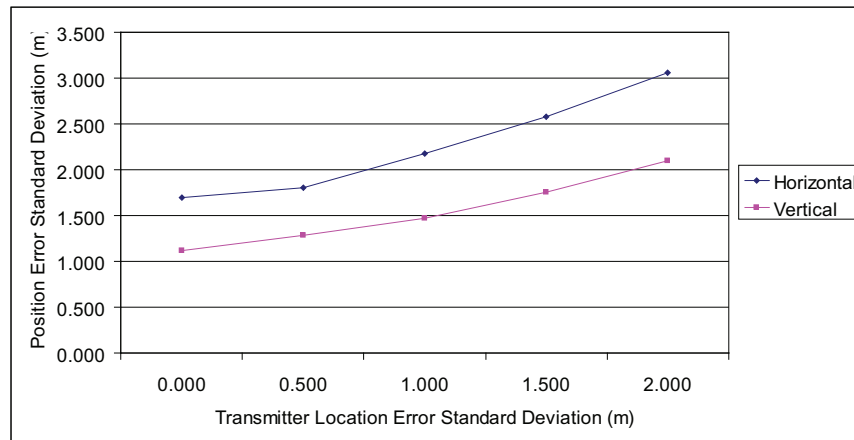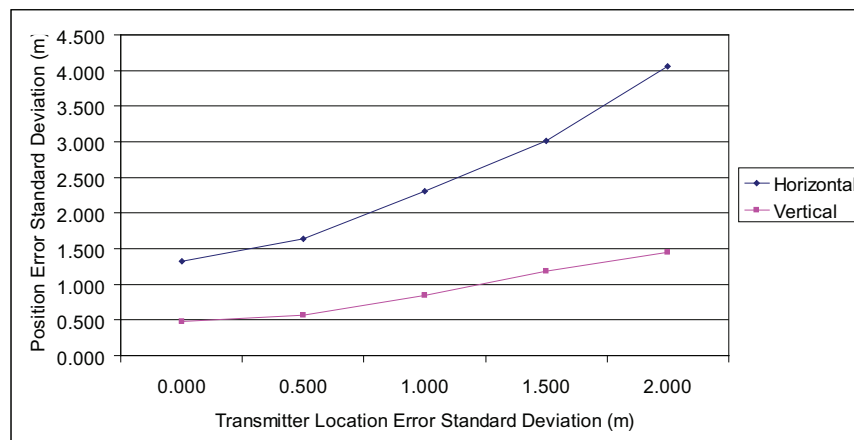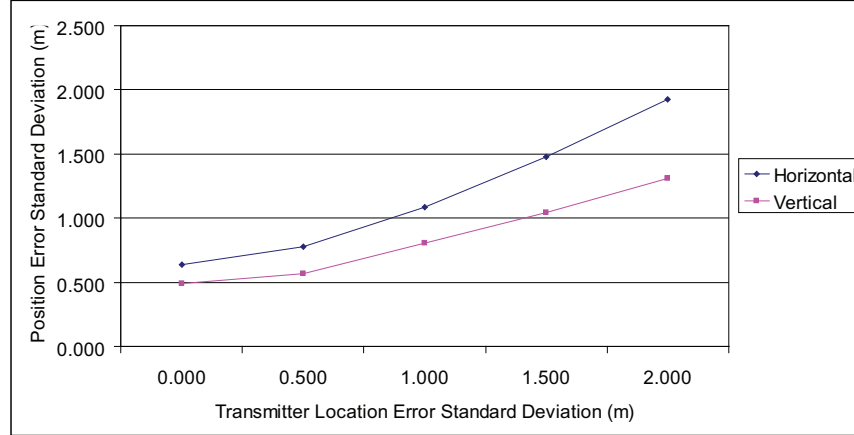Figure 4.10:   Navigation Scheme 1: Effect of location of transmitters on measurement Type III (received power vector) accuracy.

4.1.4   Trade Study 3: Vary Position of Mobile Receiver.   In a practical application, the mobile receiver will not stay stationary. The purpose of this trade study is to see how the position error standard deviation develops over a range of truth positions. Two scenarios are used to vary the x and y positions and the depth of the mobile receiver. All other parameters remain unchanged from the baseline.

The first of the two scenarios varies the x and y position in increments of 10m starting from (10,10) up to (90,90) for a total of 81 positions. Figures 4.11-4.16 show a contour for each axis position error standard deviation of the mobile as it moves through each position change. The second scenario varies the depth of the mobile from $-10m$ to $-100m$ in steps of $10m$ at the x,y position of the baseline, (50,30). Figures 4.17-4.19 give the error standard deviation results for each measurement type.

The contours for the first scenario show that the best horizontal position solutions for all three types can be found in the center of the network. This is due to the placement geometry of the transmitters. When the mobile receiver is in the center of the network, the received measurements have a high horizontal sensitivity. Any small change in the x or y position results in a large change in the measurements used to create that position. This gives rise to a smaller error estimation. As the mobile

46

moves closer to a given transmitter, the horizontal sensitivity for that transmitter decreases, thereby increasing the position error.

For the vertical solution, the vertical resolution of Types 2 and 3 follow the same trend as the horizontal resolution. However, for Type I, the vertical resolution is better as it horizontally approaches a given transmitter. This is because Type I is a length measurement. As the mobile moves underneath a transmitter, the length measurement becomes a direct translation to the vertical position. Since its vertical resolution is higher there, its position solution error will be lower.

The second scenario that varies the depth of the mobile receiver shows similar trends that the first scenario did. As the depth of the transmitter increases, the horizontal resolution decreases so the position error increases. The vertical resolutions for Types 2 and 3 also decreases as the depth increases resulting in an increased position error. For Type I, a length measurement, the vertical accuracy increases as with the first scenario. The measurements are primarily vertical so the the vertical position error decreases the further the mobile receiver goes.

4.1.5 Trade Study 4: Vary Error Sources Independently. The error sources that are associated with the measurements can affect the position solution generated by the simulation in various ways. The purpose of this Trade Study is to see how changing these error sources can affect the standard deviation of the position error.

There are five error sources that can be set for this simulation. Trade Study 2 covered one of these error sources, the location of the transmitters. The other four are raw power vector measurement errors $(\delta x, \delta y, \delta z)$, material constant μ error, material constant σ error, and the transmit power error, δP. This Trade Study will look at varying two of these errors, the raw power vector measurement errors and the material constant μ error. The remaining two errors are believed to affect the position solution in ways similar to the material constant μ error since they all affect the magnitude of the field vector measurements and not the actual direction. Table 4.4 lists the error parameters used in this Trade Study. All other parameters remain unchanged from

Figure 4.11:   Navigation Scheme 1: Horizontal position error standard deviation contour for measurement Type I in Trade Study 3.

Figure 4.12:   Navigation Scheme 1: Vertical position error standard deviation contour for measurement Type I in Trade Study 3.

Figure 4.13:   Navigation Scheme 1: Horizontal position error standard deviation contour for measurement Type II in Trade Study 3.

Figure 4.14:   Navigation Scheme 1: Vertical position error standard deviation contour for measurement Type II in Trade Study 3.
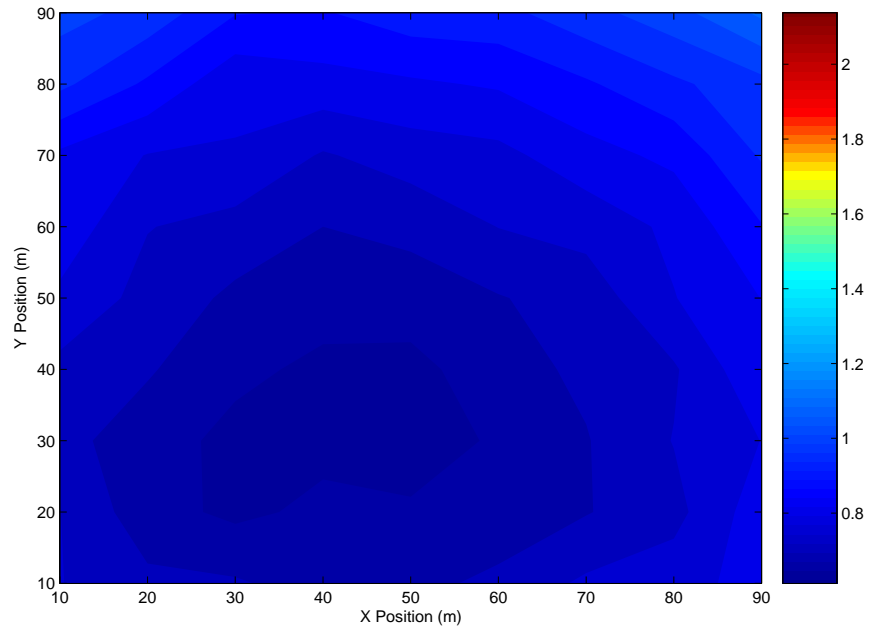
Figure 4.15:   Navigation Scheme 1: Horizontal position error standard deviation contour for measurement Type III in Trade Study 3.
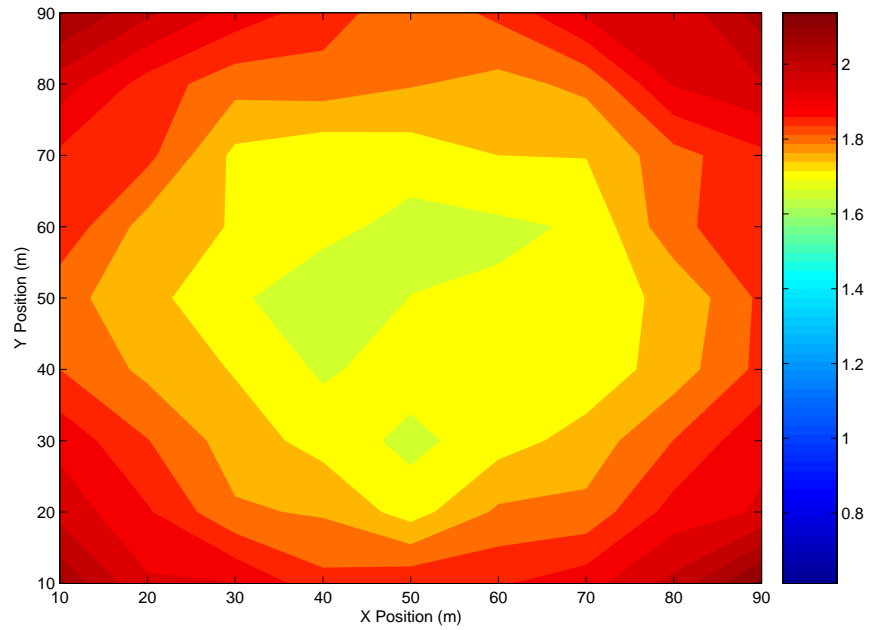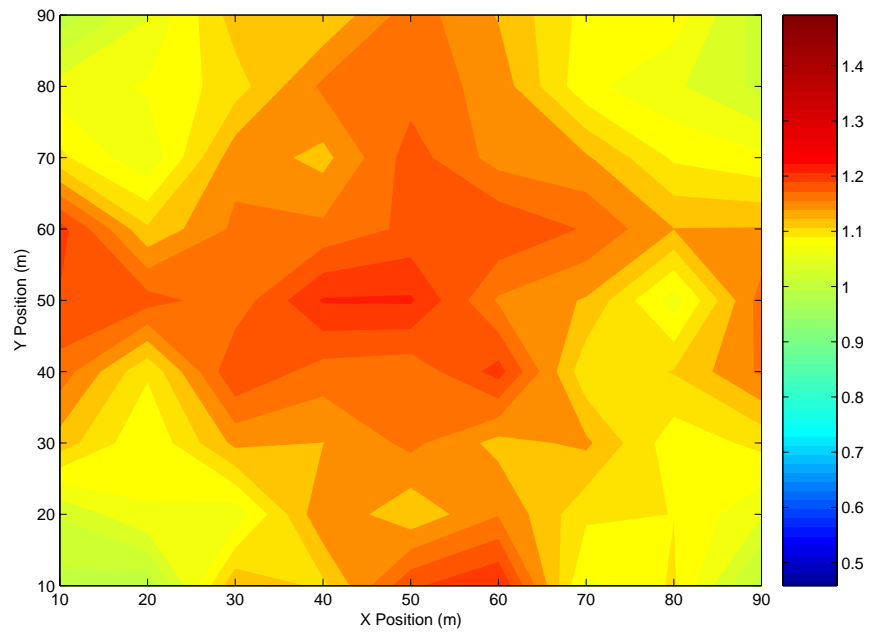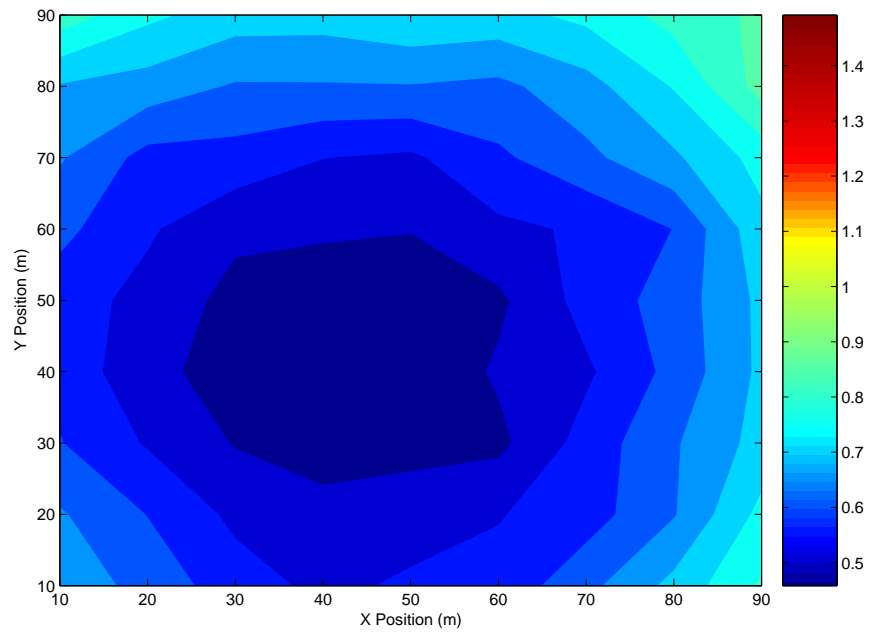

Figure 4.16:   Navigation Scheme 1: Vertical position error standard deviation contour for measurement Type III in Trade Study 3.
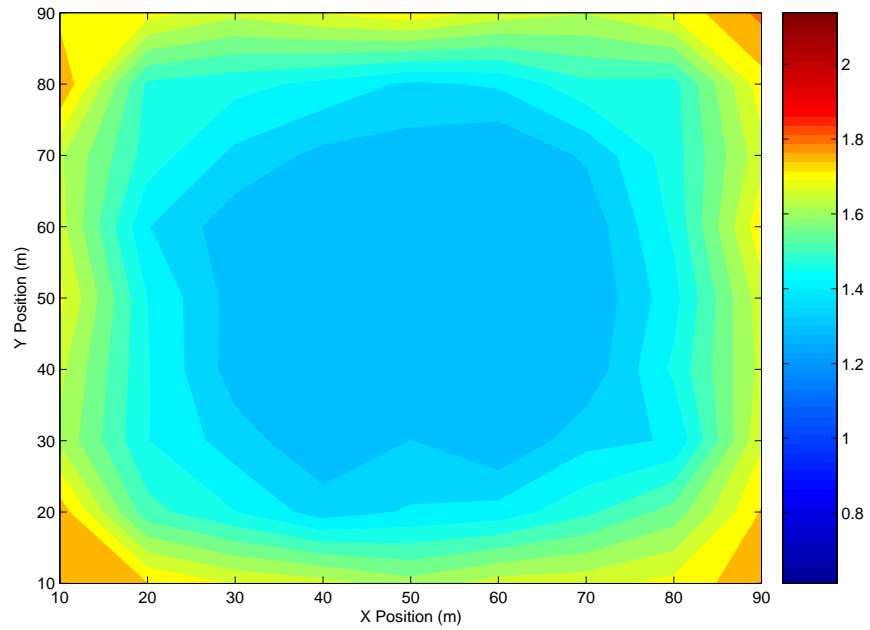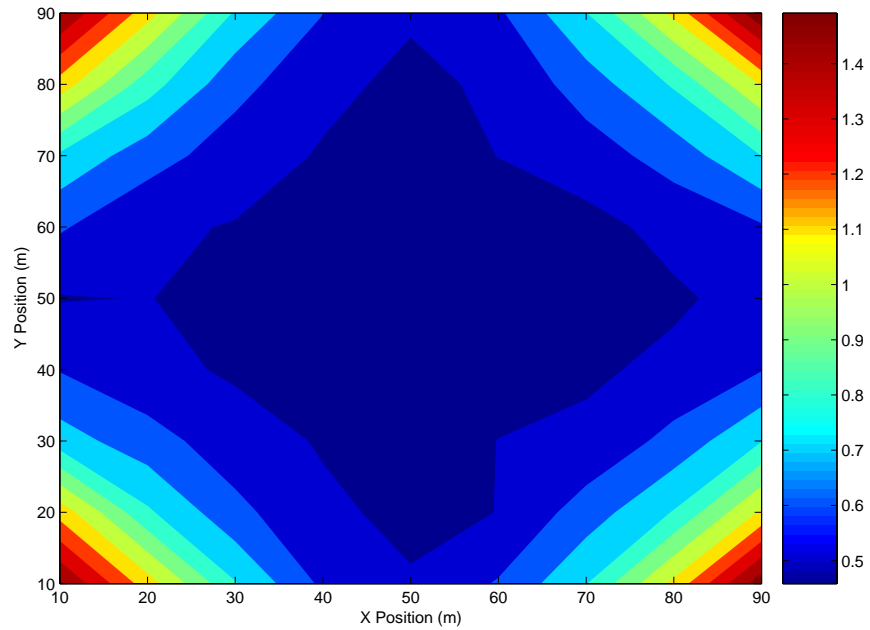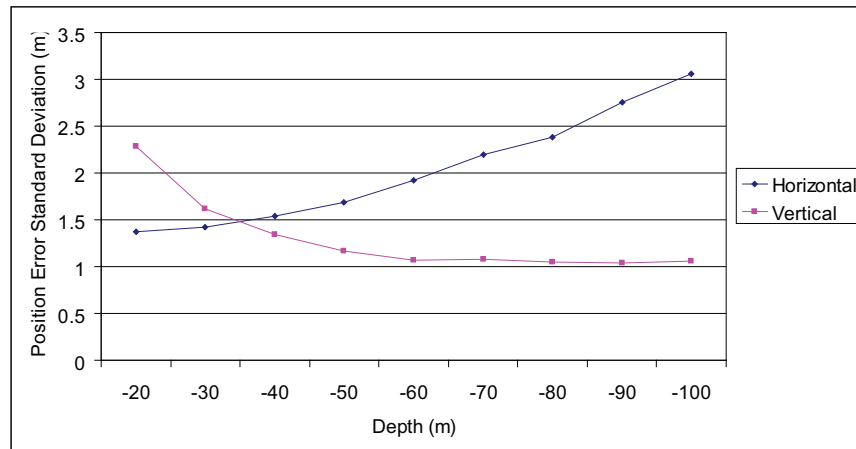
Figure 4.17:   Navigation Scheme 1: Effect of mobile receiver depths on measurement Type I (length) accuracy.

Figure 4.18:   Navigation Scheme 1: Effect of mobile receiver depth on measurement Type II (difference angle) accuracy.

51

Figure 4.19:   Navigation Scheme 1: Effects of mobile receiver depth on measurement Type III (received power vector) accuracy.

the baseline simulation. Figures 4.20-4.25 show the results for both of the errors used.

For the field vector measurement errors, the standard deviation analysis shows that the standard deviations follow a linear trend. As the error increases in each axis, so does the position error by a linear amount for the horizontal and vertical. The Type II solution method resolves a better overall vertical solution as the data is interpolated. It appears to the most robust vs. changes in the field vector measurements.

The material constant μ error source only affects the Type I solution method. This is due to the fact that Type I relies solely on the magnitude of the raw power vector measurement to create a length. As the material constant μ error increases, the error in the magnitude also increases. This shows up in the position solution error standard deviation as shown in Figure 4.23. Type II and Type III solution methods rely on the direction of the vector rather than the magnitude to determine a position solution. Therefore, the affect of the material constant μ error on Type II and Type III solution methods is negligible.

Table 4.4:   Navigation Scheme 1: Error standard deviation for error sources used in Trade Study 4.

| Test	δx_p	δy_p	δz_p	$\delta \mu$
1	0.1	0.1	0.1	0
2	0.2	0.2	0.2	0
3	0.3	0.3	0.3	0
4	0.4	0.4	0.4	0
5	0.5	0.5	0.5	0
6	0.6	0.6	0.6	0
7	0.7	0.7	0.7	0
8	0.8	0.8	0.8	0
9	0.9	0.9	0.9	0
10	1.0	1.0	1.0	0
11	0	0	0	0.025
12	0	0	0	0.050
13	0	0	0	0.075
14	0	0	0	0.100
15	0	0	0	0.125
16	0	0	0	0.150

Figure 4.20:   Navigation Scheme 1: Effect of received power vector errors on measurement Type I (length) accuracy.
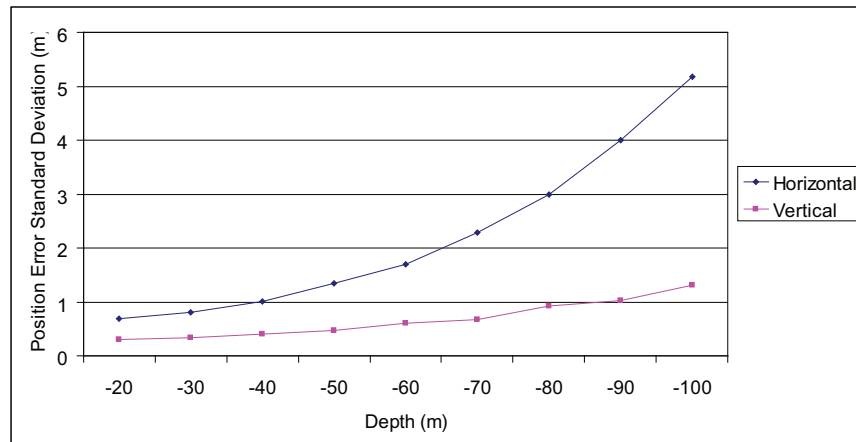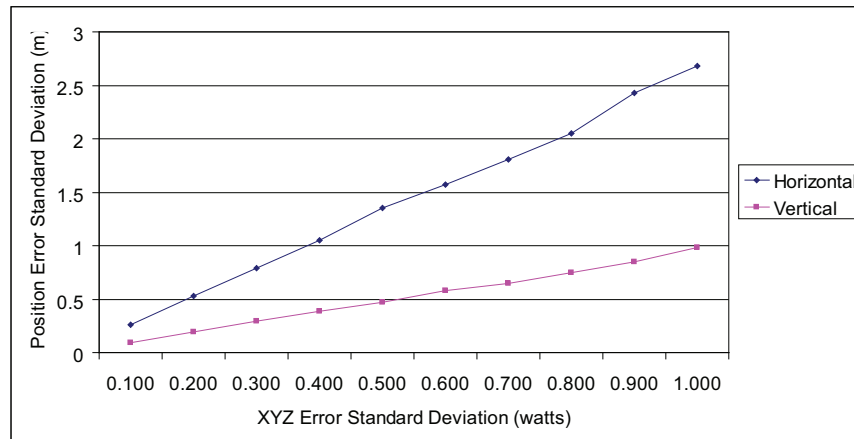
Figure 4.21: Navigation Scheme 1: Effect of received power vector errors on measurement Type II (difference angle) accuracy.
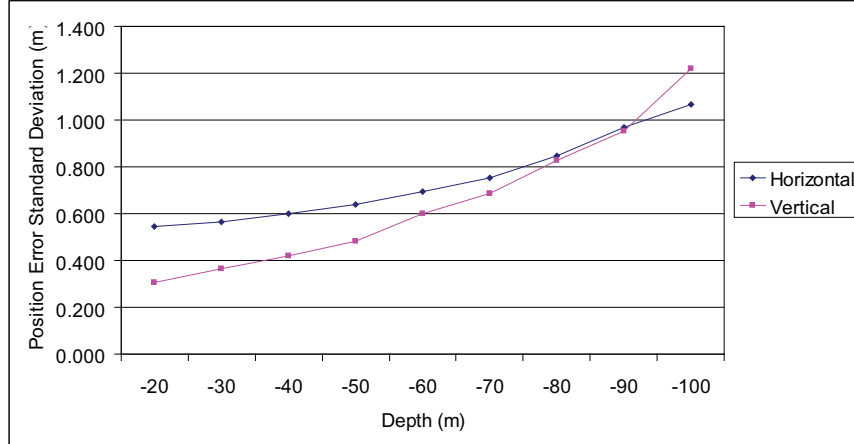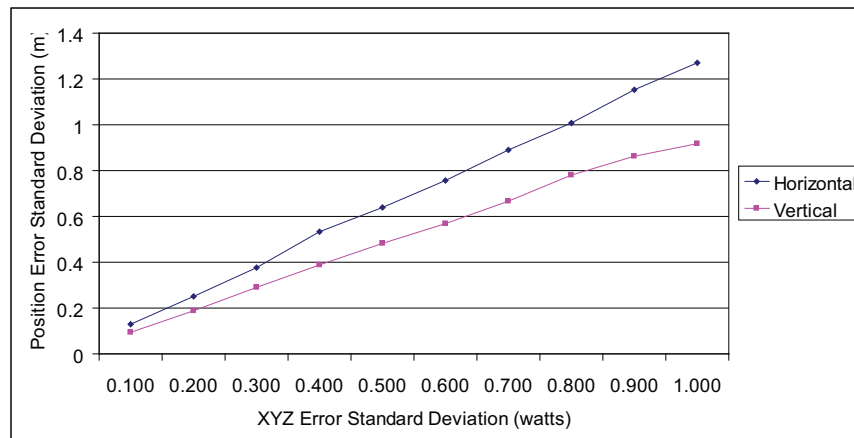

Figure 4.22: Navigation Scheme 1: Effect of received power vector errors on measurement Type III (received power vector) accuracy.
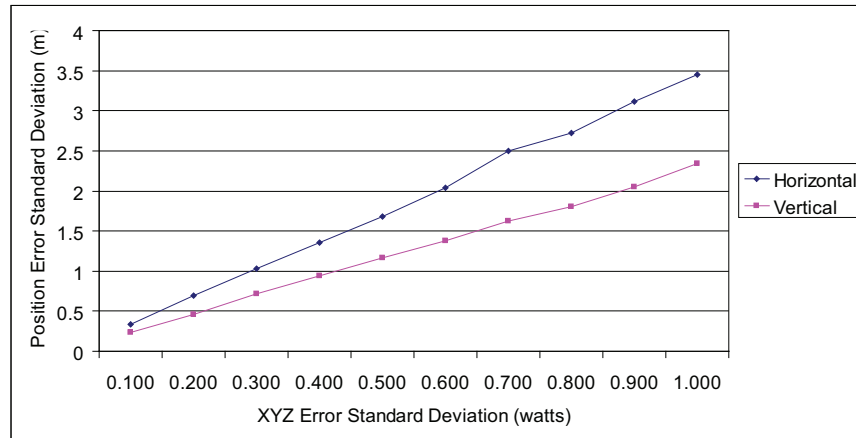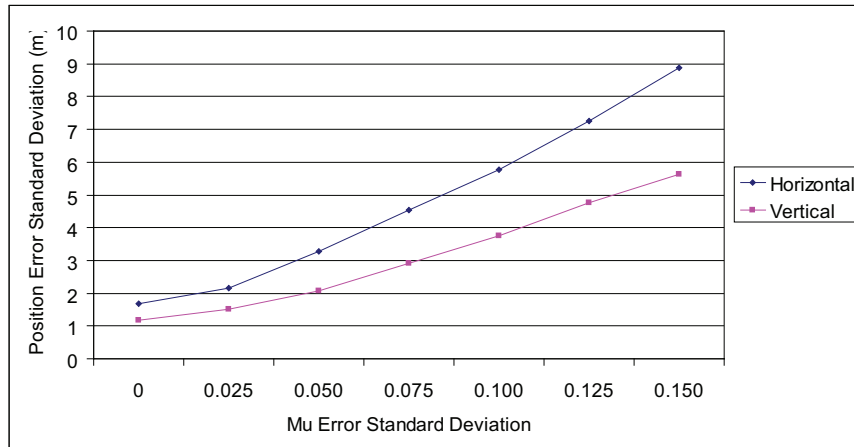
Figure 4.23:   Navigation Scheme 1: Effect of material constant μ errors on measurement Type I (length) accuracy.
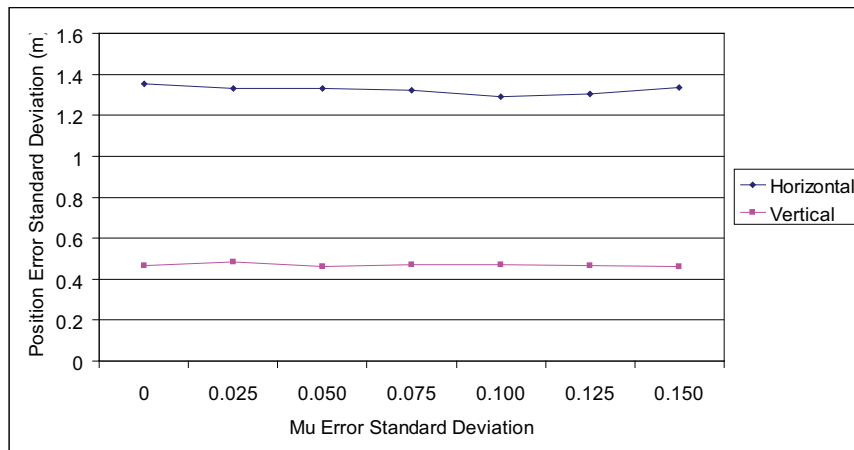
Figure 4.24:   Navigation Scheme 1: Effect of material constant μ errors on measurement Type II (difference angle) accuracy.
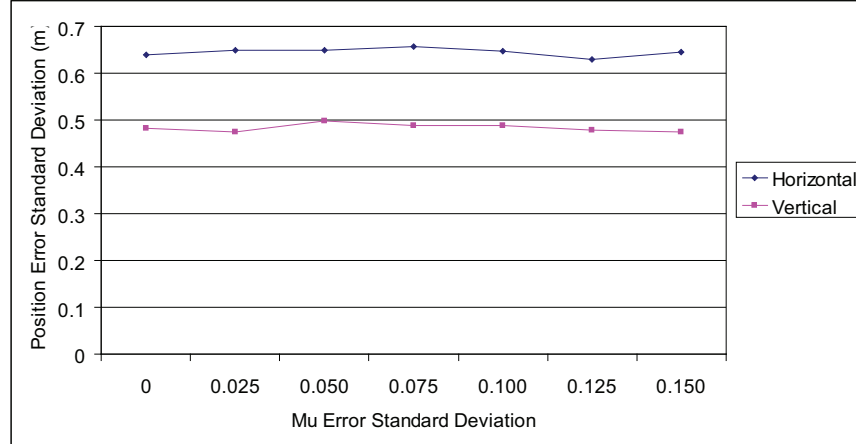
Figure 4.25: Navigation Scheme 1: Effect of material constant μ errors on measurement Type III (received power vector) accuracy.

4.2 Very-Low Frequency Data Collection System

The results and analysis for the second simulation is found in this section. The trade studies are similar to those from the previous chapter but include those specific to this simulation. These trade studies include varying the locations of the reference receivers, the position of the mobile receiver, the number of signals received, the orientation of the signals received, and the error sources involved in the simulation. A 'zero-error check' was performed on the simulation for which all errors were set to zero. This is to ensure that the simulation's algorithms are working as intended. A position solution converged with an error less than 10^{-9} from the truth.

4.2.1 Baseline Results. As in the previous section, the baseline results establish reference data to evaluate the subsequent trade studies. These results characterize the general performance of the simulation under the assumptions laid out in Chapter 1. The parameters used for the baseline simulation are given in Table 4.5. The five reference receivers are placed in a formation resembling a pentagon with a distance of 800m between each other. Since the simulation only solves for a 2-D position solution, the locations of the reference receivers are given in x and y local

Table 4.5:   Navigation Scheme 2: Baseline parameters.

Parameter	Value
Number of Reference Receivers	5
Nominal Solution (y-intercept, slope)	$(10, 1)$
Slope of Incoming Signals	1,-1
Time Difference of Arrival Measurement Error, δt	10 nsec

Table 4.6:   Navigation Scheme 2: Baseline results.

σ_x (m)	σ_y (m)	Horizontal (m)
1.659	1.620	2.319

level coordinates. For ease of visualization, the reference receivers are considered to be at ground-level.

The mobile receiver is positioned at 100 meters north and 100 meters east with a depth of -50m, $(100, 100, -50)$, although the depth is not used in any of the calculations. Two signals are used with slope orientations of 1 and -1. The time difference of arrival measurement standard deviation is set at 10 nanoseconds which equates to an approximately 3m standard deviation in length. Table 4.6 shows the results of the very-low frequency data collection system baseline simulation. A 1000 run Monte Carlo analysis was used to generate the position error standard deviation for each axis. For the baseline simulation where the measurement lines are perpendicular to each other, the x and y error standard deviations are approximately equal.

4.2.2 Trade Study 5: Vary Location of Reference Receivers.   This Trade Study is similar to Trade Study 2 in section 4.1.3. It's purpose is to see how the position error standard deviation changes as the known location of reference receivers varies by a certain error from $0\ m$ to $10\ m$. The reference receiver location used in the baseline simulation are considered the truth locations. Table 4.7 shows the reference

Table 4.7:   Navigation Scheme 2: Error standard deviation for reference receiver locations used in Trade Study 5.

Test	δx_L(m)	δy_L(m)
1	0	0
2	1	1
3	2	2
4	3	3
5	4	4
6	5	5
7	6	6
8	7	7
9	8	8
10	9	9
11	10	10

receiver location error standard deviation in each axis. No other parameters were changed from the baseline.

Figure 4.26 shows the error standard deviation of this Trade Study for each axis along with an overall horizontal error standard deviation root sum square (RSS). The position error standard deviation grows in a linear fashion for both x and y. With a reference receiver location error standard deviation of 10 m, the error grows from a horizontal error of 2.3 m up to 8.1 m. This results in approximately 0.6 m horizontal error for each 1m of reference receiver location error for this particular configuration.

4.2.3   Trade Study 6: Vary Position of Mobile Receiver.   As in section 4.1.4, the truth position of the mobile receiver needs to be varied across a range of values to see how the error standard deviation of the mobile receiver's position solution changes. The x and y positions start at $(-500, -500)$ and are incremented in steps of 100 m up to $(500, 500)$ for a total of 121 positions. All other parameters are kept the same from the baseline. Figure 4.27 shows the results of this Trade Study.
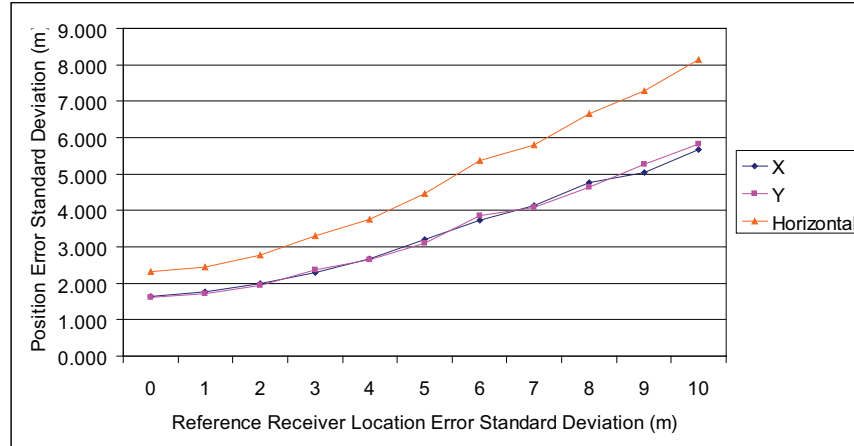
Figure 4.26:   Navigation Scheme 2: Effect of reference receivers locations on position accuracy.

The contour shows that the best position solution results can be found at the center of the network at $(0, -200)$. As the receiver moves closer to the reference receivers, the position errors increase by more than 50% from that of the center. The mobile receiver has about 1000 square meters of movement where the error standard deviation is within 0.3 m of the best solution.

4.2.4   Trade Study 7: Vary Number of Signals.   The purpose of this Trade Study is to see how the standard deviation of the mobile receiver's position changes as more signals of opportunity are received. The original signals from the baseline simulation are used with additional signals added one at a time. The orientation of the signals were chosen to give a wide range of possible outcomes. Table 4.8 lists and Figure 4.28 shows the orientation of each added signal. All other parameters from the baseline remain unchanged. The results of this Trade Study are shown in Figure 4.29.

As expected, more information about the mobile receiver's position is gained from additional signals. Therefore, the mobile receiver's position error standard deviation decreases for each axis as more signals are added. The very small difference between five and six signals shows that more than six signals would not improve the mobile receiver's position solution by a substantial margin.

59
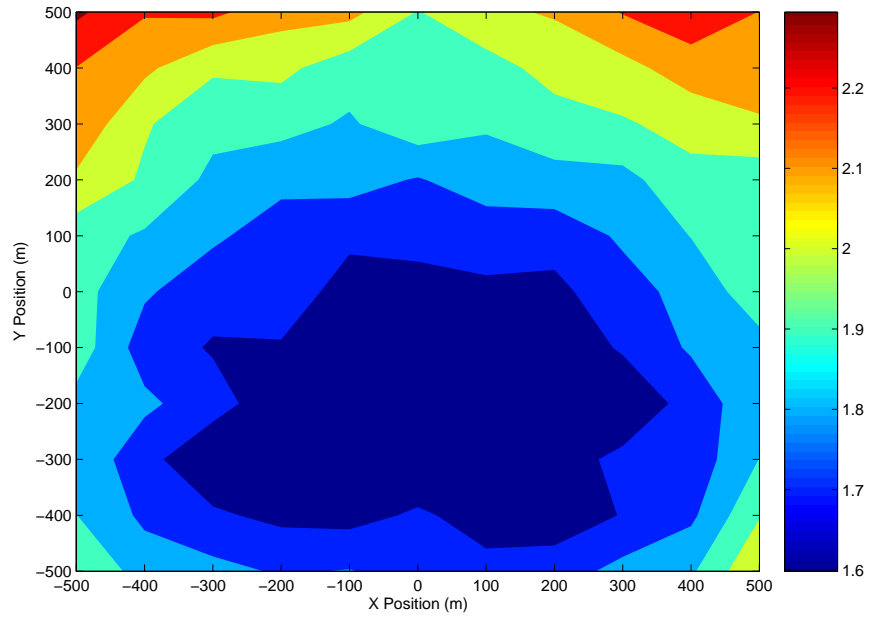
Figure 4.27: Navigation Scheme 2: Horizontal position error standard deviation contour in Trade Study 6.

Table 4.8: Navigation Scheme 2: Orientation of each added signal used in Trade Study 7.

1	2	3	4	5	6
1	-1				
1	-1	0			
1	-1	0	.5		
1	-1	0	.5	10	
1	-1	0	.5	10	-50
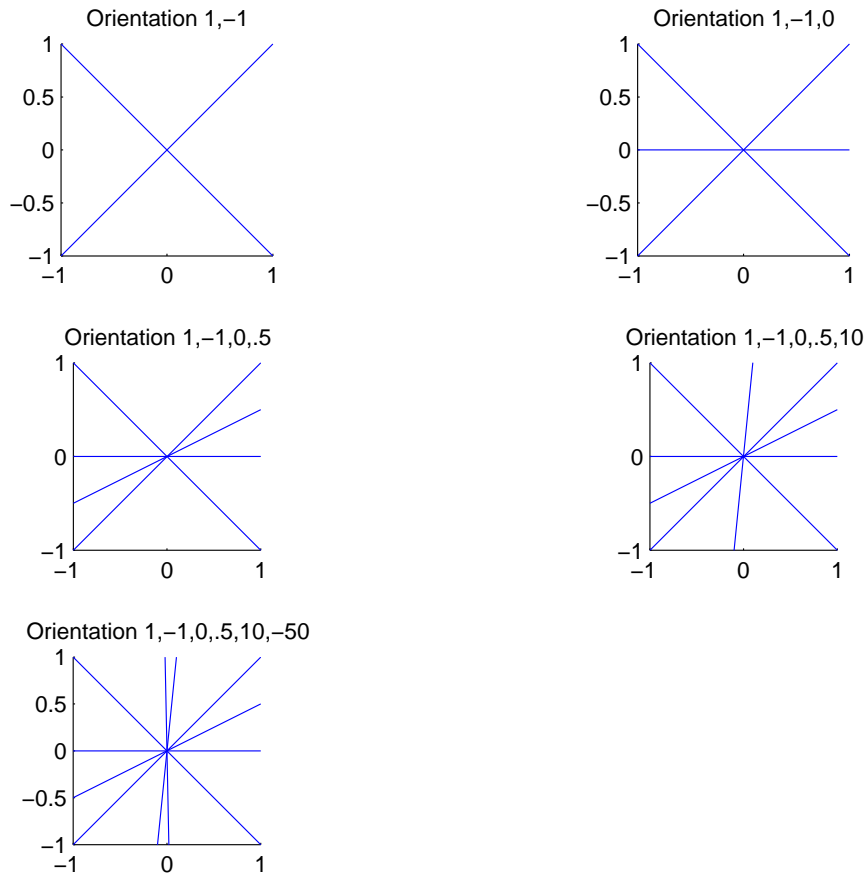
Figure 4.28:   Navigation Scheme 2: Orientation (slope) of each
added signal.
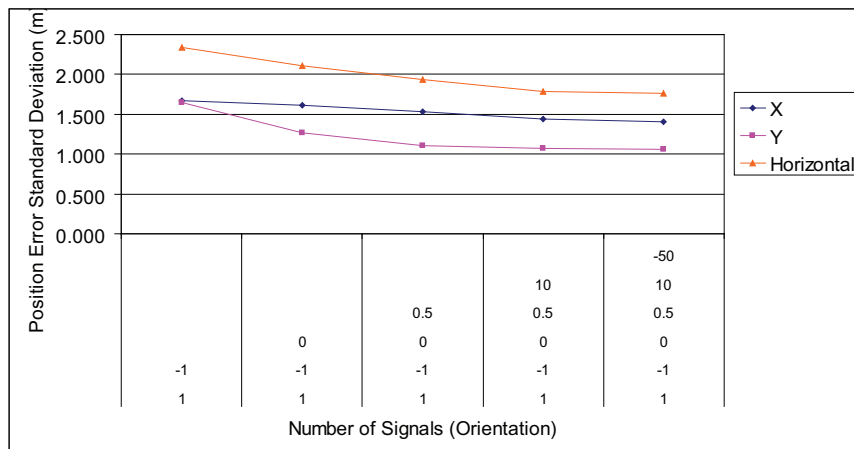
Figure 4.29:   Navigation Scheme 2: Effect of number of signals
on position accuracy.

Table 4.9:   Navigation Scheme 2:   Orientation (slope) of signals used in Trade Study 8.

Signal 1	Signal 2
-2.0	+/-1.0
-1.8	+/-1.0
-1.6	+/-1.0
-1.4	+/-1.0
-1.2	+/-1.0
-1.0	+/-1.0
-0.8	+/-1.0
-0.6	+/-1.0
-0.4	+/-1.0
-0.2	+/-1.0
0.0	+/-1.0
0.2	+/-1.0
0.4	+/-1.0
0.6	+/-1.0
0.8	+/-1.0
1.0	+/-1.0
1.2	+/-1.0
1.4	+/-1.0
1.6	+/-1.0
1.8	+/-1.0
2.0	+/-1.0
-2	+/-1.0

4.2.5   Trade Study 8: Vary Orientation of Signals.   The baseline simulation used two signals that were perpendicular to each other with orientation slopes of 1 and -1 respectively. This Trade Study will show the effect of varying either slope through a range of values. These values are shown in Table 4.9. Essentially they are each varied from -2 to 2 in increments of .2. All other parameters from the baseline remain unchanged. The results of this Trade Study are shown in Figure 4.30 and 4.31.

The data shows that the orientation of the signals does have a dramatic affect on the mobile receiver's position error standard deviation. In both cases, as the slope of the second signal approached that of the first, the error standard deviation
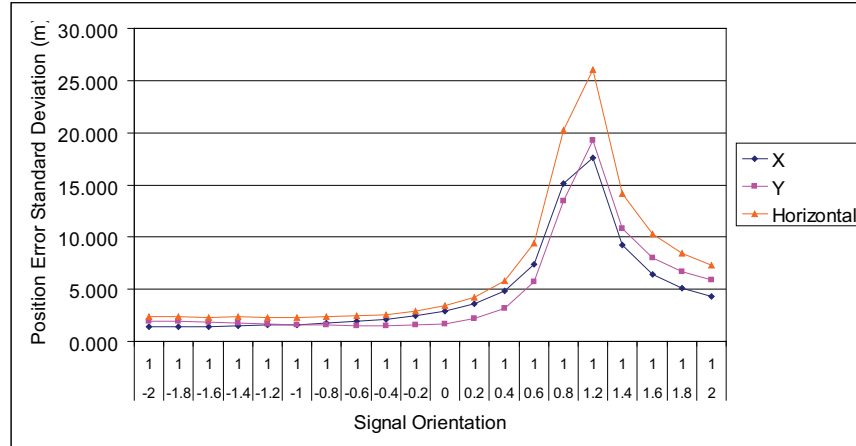
Figure 4.30:   Navigation Scheme 2: Effect of signal orientation
with constant slope of 1 on position accuracy.
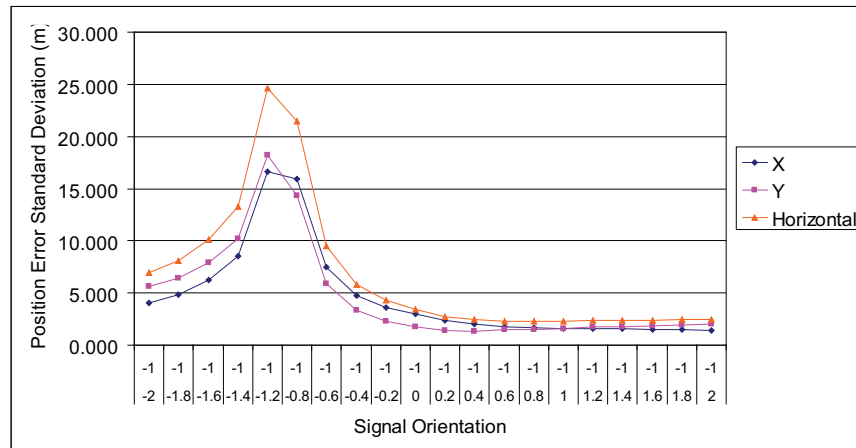
Figure 4.31:   Navigation Scheme 2: Effect of signal orientation
with constant slope of -1 on position accuracy.

exponentially increased to infinity as the slopes became equal. As the slopes became
further apart, the standard deviation began to mirror the results found in the baseline.
This could have a serious impact on the position solution if two signals from the same
source was used as their orientation would be equal. The ideal situation would be for
signals to come in from orthogonal directions.

4.2.6   Trade Study 9: Vary Error Source.   The purpose of this Trade Study
is to see how varying the error added to the measurements generated from each signal
affects the standard deviation of the mobile receiver's position solution. The baseline

63

Table 4.10: Error standard deviation for error sources used in Trade Study 9.

Test	δt
1	10 nsec
2	20 nsec
3	30 nsec
4	40 nsec
5	50 nsec
6	60 nsec
7	70 nsec
8	80 nsec
9	90 nsec
10	100 nsec

simulation used a 10 nanosecond standard deviation for the error added to each time difference of arrival measurement. This is equivalent to approximately 3 meters of error. This Trade Study increments the standard deviation by 10 nanoseconds up to 100 nanoseconds, or approximately 30 meters of error, as shown in Table 4.10. All other parameters are left unchanged from the baseline. Figure 4.32 shows the results of the Trade Study.

The error standard deviation of the mobile receiver's position solution follows a linear progression as the standard deviation of the error added to the time difference of arrival measurements is increased. At ten times the error added, the error standard deviation of the mobile receiver's position solution also increases by a factor of ten. Now a relationship between the error added to the time difference of arrival measurements and the error in the mobile receiver's position solution can be made. Multiplying the measurement error by a certain factor will multiply the error of the position by the same amount.

4.3 Summary

This chapter presented the results and analysis of the baseline simulations and trade studies for both schemes implemented in this research. The baselines showed

64
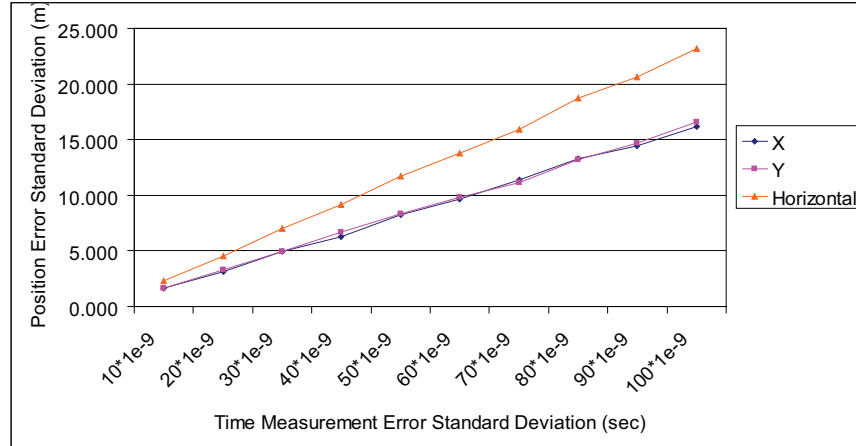
Figure 4.32: Navigation Scheme 2: Effect of time measurement error on position accuracy.

that a position solution could be found with an associated standard deviation under the assumptions given in Chapter 1. Each Trade Study then expanded the baselines to vary several parameters, keeping the rest the same. The trade studies attempted to cover various situations in which a position solution may be needed and found trends in the associated error standard deviation. Chapter 5 will give some conclusions based on these findings and make recommendations for future research.

V. Conclusions and Recommendations

This chapter highlights overall conclusions and recommendations for the research. The results for both simulated underground navigation schemes are summarized and conclusions provided. Recommendations for future research that relate to or expand upon this research are then presented.

5.1 Summary of Results

Each navigation scheme was implemented in MATLAB® as outlined in Chapter 3 and brought about varying results as discussed and analyzed in Chapter 4. This section summarizes the results presented in this thesis.

5.1.1 Transmitter/Receiver Scheme.

The simulation of this scheme was broken down into blocks detailing the methods used to find a position solution and the associated error. User defined parameters initialized the simulation and were fed directly into the truth model. Received raw power vector measurements (Type III measurement) were generated and converted to a length (Type I measurement) and difference angle (Type II measurement) between the mobile receiver and the transmitters. All three types of measurements were then used in a least squares iteration technique or line fit to solve for the mobile receiver's position.

A baseline simulation was established using four surface transmitters arrayed in a square formation. The mobile receiver was positioned at $(x = 50, y = 30, z = -50)$ receiving measurements with a standard deviation of 0.5 watts. Parameters used in the baseline simulation showed Type III measurements having the best horizontal solution but required the use of an Inertial Navigation System (INS). Without the INS, Type II measurements provided a 20% horizontal improvement over Type I measurements and a vertical improvement of 150%. Four trade studies (one through four) were used to vary certain user defined parameters so that the position solution accuracy could be analyzed in different scenarios.

The first trade study varied the number of transmitters from the baseline case of four to three, five, and six. The results showed that as the number of transmitters is increased, the error standard deviation of the mobile receiver's position solution decreased giving a more accurate solution. The second trade study varied the assumed location of the transmitters from a standard deviation of 0 m up to 2 m. Type III still provided the best performance over the range used in the study. However, Type I appears to be the most robust to transmitter location errors as the data is interpolated to higher transmitter location errors. The third trade study moved the mobile receiver over a range of positions. The results show that the best horizontal position solution for all types of measurements occurred in the center of the transmitter network. Type I measurements had the best vertical position solution as the depth increased from -10 m to -100 m. The forth trade study varied the errors in the material constant μ and the received power vector used to create the measurements. The material constant μ only had an affect on Type I measurements for this trade study. The received power vector measurement error brought about a linear change in the error standard deviation of the mobile receiver's position.

5.1.2 VLF Data Collection System. The simulation for VLF data collection system was set up similar to the transmitter/receiver scheme. User defined parameters initialized the simulation and were fed directly into the truth model. Time-difference-of-arrival (TDOA) between the reference receivers and the mobile receiver measurements were generated from the parameters and truth model. The position solution was a line that fit the measurements through a least squares iteration technique. The mobile receiver's 2-D position was assumed to be somewhere along this line. As additional measurements were added, the mobile receiver's position resolved as a weighted least squares intersection of the lines.

A baseline simulation was also established for this scheme with five reference receivers arrayed in a pentagon formation. The mobile receiver was positioned at the $(x = 100, y = 100)$ received two signals of opportunity. Each signal generated five

TDOA measurements with a standard deviation of 10 nsec. The baseline showed that the x and y standard deviations for the mobile receiver's position were approximately equal around 1.65m. Five trade studies (five through nine) were used with this scheme to analyze the error standard deviation of the position solution in different scenarios.

The fifth trade study varied the reference receiver locations in a similar way that trade study one varied the transmitter locations. The results showed a 0.6 m horizontal standard deviation for each 1m of reference receiver location error standard deviation. The sixth trade study moved the mobile receiver over a range of positions similar to trade study three. The results show that the best position solution can be found at the center of the network at $(x = 0, y = -200)$. The seventh trade study varied the number of incoming signals received through the network. As more signals are received, the accuracy of the position solution increases. The eighth trade study varies the orientation of one incoming signal over a range of values while keeping the other fixed. The data shows that the relative orientation between two incoming signals dramatically affects the position solution accuracy. As the signals move closer together and become parallel, the error standard deviation of the mobile receiver's position solution grows exponentially. As the signals move further apart to become orthogonal, the error standard deviation converges to the baseline results. The ninth and final trade study varied the time-difference-of-arrival measurement error. The results show that a linear relationship between the measurement error standard deviation and the mobile receiver's error standard deviation exists.

5.2   Recommendations for Future Research

The scope of this research was to create a simulation that would take incoming measurements and use them to find a position solution and associated standard deviation. To further extend this research, recommendations are made in this section concerning the simulation and a hardware implementation.

There were a number of assumptions made for this research that may not be applicable in a real-world environment. The simulated model fidelity was restricted by

these assumptions. The simulation was a "bare-bones" attempt at incorporating basic real-world phenomena. The foundation can built upon as the modelling becomes more complex and mathematically rigorous. Listed below are four suggested improvements to the simulation:

- Underground Electromagnetic Wave Propagation Advances: The use of a linear, isotropic, and homogenous media in the transmitter/receiver scheme made possible the use of a simplified skin depth formula. It also allowed the measurements to ignore second and higher-order affects from propagating through irregular media. One obvious step, however complex, is to more adequately model the effects the Earth has on a propagating EM wave. The power vector received by the mobile transmitter could use these more complicated models to possibly remove the affects or account for them in ways this simulation did not.

- Parameter Advances: Although certain constants were used to simulate real-world values, parameters such as material constants, transmission power, received power, and transmission frequency are only approximations. An in-depth study could be performed to find a range of values for various scenarios and update the simulation accordingly.

- Clock Error Estimation: For systems that rely on timing, estimating the clock error inherent in all clocks is essential. Including clock error estimation in the algorithm could further improve the simulation accuracy.

- Kalman Filter Addition: The solution methods for this research use batch least squares techniques along with some intermediate calculations to solve for a position solution. In order to gain complete navigation information for speed and heading, a Kalman filter could be implemented to use new measurements as they arrive to update the position and velocity. A model of the mobile receiver's dynamics and a different solution method than iterative least squares would be needed to accomplish this.

In order to gain insight into what models, parameters, or solution methods need to be used, it would be beneficial to run real-world hardware tests to see exactly how the algorithms would perform. One recourse is to build a prototype system created under the assumptions presented in this research for each scheme and see where there may be problems. Appendix A illustrates a possible hardware implementation of the VLF Data Collection System.

Appendix A. Hardware Implementation Block Diagram

The hardware proposed for the VLF data collection system consists of the following:

- WR-3 VLF Radio: radio receiver configured to pick up signals from 3 kHz to 15 kHz

- GPS Receiver: standard off-the-shelf GPS receiver with data out

- Data Acquisition Device: data sampled at 2 MHz for better resolution of low frequency signals

- Computer Laptop: used for data processing and control of the data acquisition device

- Power Supply (not shown): provides enough power to run system for 8 hours continuously

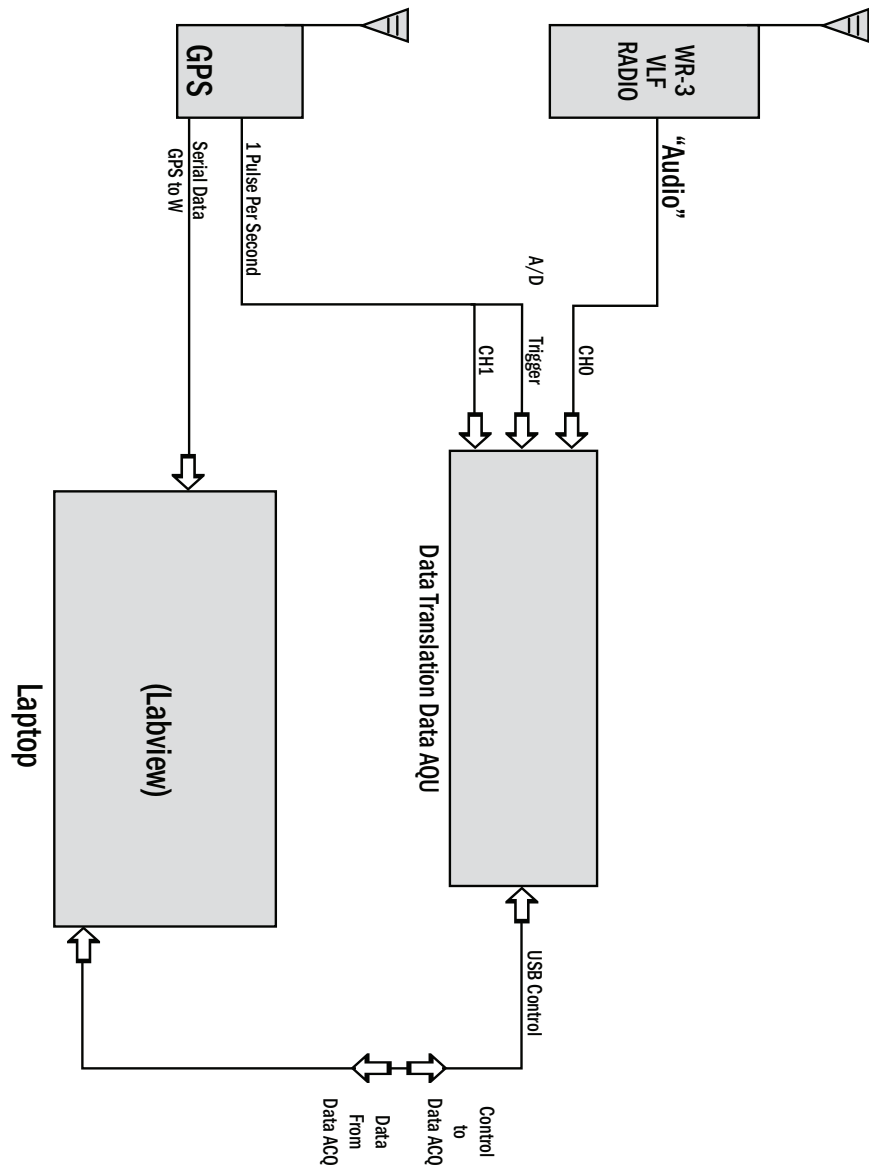Figure A.1 shows a block diagram of the VLF data collection system.

Figure A.1: Proposed VLF data collection system hardware setup block diagram.

Bibliography

1. Cheng, D.K. *Field and wave electromagnetics.* Addison-Wesley Reading, 1983.

2. Cummer, S. "Ionospheric D region remote sensing using VLF radio atmospherics". *Radio Science*, 33(6):1781–1792, 1998.

3. Eggert Second Lieutenant USAF, R. J. *Evalutating the Navigation Potential of the National Television System Committee Broadcast Signal.* Master's thesis, Graduate School of Engineering, Air Force Institute of Technology (AETC), Wright-Patterson AFB OH, March 2004. AFIT/DS/ENG/04-08.

4. INFO, C.P. "RadioLocation Accuracy-Theory & Practice". *Journal (includes newssheet)*, 8:10–00.

5. Lin, C.F. *Modern navigation, guidance, and control processing.* Prentice Hall Englewood Cliffs, NJ, 1991.

6. Maybeck, P.S. *Stochastic Models, Estimation, and Control (Vols. I and II).* New York: Academic Press, 1979.

7. McEllroy Lieutenant USN, J. A. *Navigation Using Signals of Opportunity in the AM Transmission Band.* Master's thesis, Graduate School of Engineering, Air Force Institute of Technology (AETC), Wright-Patterson AFB OH, September 2006. AFIT/GAE/ENG/06-04.

8. Prigge, EA and JP How. "Signal architecture for a distributed magnetic local positioning system". *Sensors Journal, IEEE*, 4(6):864–873, 2004.

9. Strang, G. and K. Borre. *Linear Algebra, Geodesy, and GPS.* Cambridge Press Wellesley, 1997.

10. Tsujimura, T., S. Shirogane, T. Manabe, and M. Matsumoto. "Electromagnetic navigation system for underground tunneling robot". *Systems, Man, and Cybernetics, 1999. IEEE SMC'99 Conference Proceedings. 1999 IEEE International Conference on*, 4, 1999.

REPORT DOCUMENTATION PAGE

The public reporting burden for this collection of information is estimated to average 1 hour per response, including the time for reviewing instructions, searching existing data sources, gathering and maintaining the data needed, and completing and reviewing the collection of information. Send comments regarding this burden estimate or any other aspect of this collection of information, including suggestions for reducing this burden to Department of Defense, Washington Headquarters Services, Directorate for Information Operations and Reports (0704–0188), 1215 Jefferson Davis Highway, Suite 1204, Arlington, VA 22202–4302. Respondents should be aware that notwithstanding any other provision of law, no person shall be subject to any penalty for failing to comply with a collection of information if it does not display a currently valid OMB control number. **PLEASE DO NOT RETURN YOUR FORM TO THE ABOVE ADDRESS.**

1. REPORT DATE (DD–MM–YYYY)	2. REPORT TYPE	3. DATES COVERED (From — To)
22–03–2007	Master's Thesis	Sept 2006 — Mar 2007

4. TITLE AND SUBTITLE	5a. CONTRACT NUMBER

Sub-Surface Navigation
Using Very-Low Frequency
Electromagnetic Waves

5b. GRANT NUMBER

5c. PROGRAM ELEMENT NUMBER

6. AUTHOR(S)

5d. PROJECT NUMBER

Alan L. Harner,1st Lt, USAF

5e. TASK NUMBER

5f. WORK UNIT NUMBER

7. PERFORMING ORGANIZATION NAME(S) AND ADDRESS(ES)

Air Force Institute of Technology
Graduate School of Engineering and Management
2950 Hobson Way
WPAFB, OH 45433-7765

8. PERFORMING ORGANIZATION REPORT NUMBER

AFIT/GE/ENG/07-12

9. SPONSORING / MONITORING AGENCY NAME(S) AND ADDRESS(ES)

Dr. Mikel M. Miller, Ph.D. (937) 255-6127x4274
AFRL/SNRP
Bldg 620, Room 3AJ39
2241 Avionics Circle
WPAFB, OH 45433-7333
email: mikel.miller@wpafb.af.mil

10. SPONSOR/MONITOR'S ACRONYM(S)

11. SPONSOR/MONITOR'S REPORT NUMBER(S)

12. DISTRIBUTION / AVAILABILITY STATEMENT

APPROVED FOR PUBLIC RELEASE; DISTRIBUTION UNLIMITED

13. SUPPLEMENTARY NOTES

14. ABSTRACT

This research proposes two schemes utilizing very-low frequency (VLF) electromagnetic waves to navigate underground. The first scheme consists of using above-ground beacon transmitters to broadcast VLF signals to an underground mobile receiver which uses methods such as triangulation and trilateration to obtain a position solution. The second scheme consists of using above-ground reference receivers along with an underground mobile receiver to form time-difference-of-arrival measurements of incoming VLF signals of opportunity, such as lightning strike emissions, to calculate a position solution. The objective of this thesis is to develop positioning algorithms and use simulations as a tool to characterize the effects that varying parameters such as measurement errors, measurement type, number of measurements, transmitter/ reference receiver location, mobile receiver position, and material constant errors have on the accuracy of a position solution. The results show trends that would still be expected using more complex methods and models.

15. SUBJECT TERMS

Underground Navigation, Beacon Navigation, Signals of Opportunity, TDOA, Triangulation, Trilateration, Geolocation

16. SECURITY CLASSIFICATION OF:			17. LIMITATION OF ABSTRACT	18. NUMBER OF PAGES	19a. NAME OF RESPONSIBLE PERSON
a. REPORT	b. ABSTRACT	c. THIS PAGE			Dr. John F. Raquet
U	U	U	UU	87	19b. TELEPHONE NUMBER (include area code) (937) 255–3636, ext 4580 john.raquet@afit.edu